

Prediction-Augmented Trees for Reliable Statistical Inference

Vikram Kher^{*1}, Argyris Oikonomou[†], and Manolis Zampetakis^{‡1}

¹Department of Computer Science, Yale University

October 21, 2025

Abstract

The remarkable success of machine learning (ML) in predictive tasks has led scientists to incorporate ML predictions as a core component of the scientific discovery pipeline. This was exemplified by the landmark achievement of AlphaFold (Jumper et al. (2021)). In this paper, we study how ML predictions can be safely used in statistical analysis of data towards scientific discovery. In particular, we follow the framework introduced by Angelopoulos et al. (2023). In this framework, we assume access to a small set of n gold-standard labeled samples, a much larger set of N unlabeled samples, and a ML model that can be used to impute the labels of the unlabeled data points. We introduce two new learning-augmented estimators: (1) *Prediction-Augmented Residual Tree (PART)*, and (2) *Prediction-Augmented Quadrature (PAQ)*. Both estimators have significant advantages over existing estimators like PPI and PPI++ introduced by Angelopoulos et al. (2023) and Angelopoulos et al. (2024), respectively.

PART is a decision-tree based estimator built using a greedy criterion. We first characterize PART’s asymptotic distribution and demonstrate how to construct valid confidence intervals. Then we show that PART outperforms existing methods in real-world datasets from ecology, astronomy, and census reports, among other domains. This leads to estimators with higher confidence, which is the result of using both the gold-standard samples and the machine learning predictions.

Finally, we provide a formal proof of the advantage of PART by exploring PAQ, an estimation that arises when considering the limit of PART when the depth its tree grows to infinity. Under appropriate assumptions in the input data we show that the variance of PAQ shrinks at rate of $O(N^{-1} + n^{-4})$, improving significantly on the $O(N^{-1} + n^{-1})$ rate of existing methods.

^{*}vikram[ker]@yale.edu

[†]ar[economou]@outlook.com

[‡]manolis[zampetakis]@yale.edu

1 Introduction

Following the breakthrough development of machine learning (ML) methods over the last decade, virtually every scientific discipline has embraced ML as a method to accelerate scientific discovery by allowing faster data analysis, hypothesis generation, and experiment design [55]. A plethora of recent work demonstrates ML-enabled advances across the biological sciences (e.g, [21, 35, 43, 50, 51]), the physical sciences (e.g, [16, 33, 39, 49]), and the social sciences (e.g, [17, 30, 32, 47]). A landmark recognition of this trend came with the 2024 Nobel Prize in Chemistry, which was awarded in part for the creation of AlphaFold, a machine learning model that predicts the three-dimensional structure of a protein based on its amino acid sequence [27, 31].

One of the most profound uses of ML methods in scientific discovery can be abstractly described as follows: suppose that a scientist would like to estimate the mean value of some protein structure. At their disposal, they have access to a small set of gold-standard labeled samples $(X_i, Y_i)_{i=1}^n$ drawn from a joint distribution $P_{X,Y}$. Here, X_i represents some easily available features of the protein and Y_i denotes the structural property of interest, which is expensive to measure experimentally. Since features are easy to obtain, the researcher also has access to a much larger set of unlabeled samples $(\tilde{X}_i)_{i=1}^N$ drawn from the marginal distribution P_X , along with a black box ML model $f(X)$, e.g., AlphaFold, that predicts labels based on input features. The scientist would like to leverage the unlabeled samples and the ML model f to construct a valid confidence interval (CI) for the mean protein structure that is tighter than if they only used the labeled data.

A proposed solution to this setup was put forth by Angelopoulos et al. [4], who present a method called *Prediction Powered Inference* (PPI). The PPI estimator for the mean is defined by

$$\hat{\mu}_{\text{PPI}} = \underbrace{\mathbb{E}_N[f(\tilde{X})]}_{\text{estimate of mean}} + \underbrace{\mathbb{E}_n[Y - f(X)]}_{\text{estimate of bias / residual}},$$

where \mathbb{E}_n and \mathbb{E}_N denote the empirical expectations over the labeled and unlabeled samples, respectively. Angelopoulos et al. [4] showed that the PPI estimator is unbiased and, when the model f is accurate, achieves lower variance than the traditional sample mean estimator of $\hat{\mu}_E = \mathbb{E}_n[Y]$. To be more precise, since $N \gg n$, the variance of the PPI estimator, and consequently the width of the confidence interval, is primarily determined by

$$\text{Var}[\hat{\mu}_{\text{PPI}}] \approx \frac{\text{Var}[Y - f(X)]}{n} \quad \text{compared to} \quad \text{Var}[\hat{\mu}_E] = \frac{\text{Var}[Y]}{n}.$$

Intuitively, if the model $f(x)$ is a good predictor of $\mathbb{E}[Y|X]$, then we expect that $\text{Var}[Y - f(X)]$ will be smaller than $\text{Var}[Y]$. Put in another way, we expect PPI to perform well when f explains some of the variance of Y .

While PPI has demonstrated the potential of integrating ML predictions into statistical inference, significant gaps remain in understanding how we can best leverage unlabeled samples and ML models for statistical inference. Specifically, it is natural to ask the following question:

Question: *Does there exist learning-augmented estimators that offers tighter confidence intervals compared to existing approaches?*

Our Contributions. We make progress towards answering this question by developing two novel estimation methods: the *Prediction-Augmented Residual Tree (PART)* estimator and the *Prediction-Augmented Quadrature (PAQ)* estimator. Compared to PPI and its refinement PPI++, PART produces consistently tighter confidence intervals; whereas, PAQ achieves asymptotically faster shrinkage of interval width compared PPI/PPI++. We state our contributions precisely below.

1. **Prediction-Augmented Residual Tree (Section 4).** Our first contribution is defining the PART estimator. At a high-level, the PART estimator partitions the feature space into homogeneous regions by recursively building a binary tree estimator, inspired by [13] but adapted to our setting. Each split in the tree is greedily chosen to minimize a variance-based objective function resembling the CART criterion from Breiman [11]. After the estimation tree is grown, PART computes a refined debiasing term by carefully combining estimates of mean residual in each leaf. Importantly, if we fix the depth of the PART tree to zero, our estimator coincides with PPI; thus, by appropriately tuning PART’s depth parameter, we are guaranteed to always perform at least as well as PPI. Once we define our PART estimator we proceed with the following steps.
 - (a) **Inference with PART (Sections 4.1 and 4.2).** One of the main challenges of using more complicated techniques, such as tree estimators, in simple statistical tasks is that we need to find a mathematically rigorous way to compute confidence intervals from these estimators. In our Theorems 1 and 2 we characterize the asymptotic distribution of PART and show how to construct valid confidence intervals for both the mean and linear regression coefficients.
 - (b) **Empirical Performance of PART (Section 5).** Based on the methodology that we have developed in part (a), we evaluate the confidence intervals produced by PART on several real-world datasets (including those used in [4, 5]), demonstrating markedly smaller confidence intervals compared to PPI and PPI++ while maintaining nominal coverage.
2. **PART with Deterministic Response Variable (Section 6).** Our next contribution is to introduce the PAQ estimator, which is motivated by analyzing the PART estimator in the extreme scenario where Y is a deterministic function of X , and each leaf contains only two points. We show that in this scenario, the estimation of the residual can be expressed as an integral over the feature space. This observation enables us to approximate this term using numerical quadrature techniques. Under smoothness assumptions on the residual function $r(x) = y(x) - f(x)$, we prove that PAQ’s variance shrinks at a rate of $O(N^{-1} + n^{-4})$, improving over the $O(N^{-1} + n^{-1})$ rate of PPI/PPI++.

Road Map. In Section 2, we define our model and the basic statistical framework necessary for our analysis. In Section 3, we provide a warm-up example and estimator that demonstrates how clustering can produce a debiasing term with lower variance compared to PPI or PPI++. Then we proceed in Sections 4 to 6 with the main results of the paper as we explained above.

1.1 Related Works

ML Predictions for Mean Estimation. We briefly survey the relevant landscape of using ML predictions for statistical inference. Angelopoulos et al. [4] formalized the model for prediction powered statistical inference and proposed the PPI estimator for mean estimation, linear regression coefficient estimation, odds-ratio estimation, among other targets. In follow-up work, Angelopoulos et al. [5] introduced PPI++, which uses a power-tuning parameter to adaptively down-weight the influence of the predictions based on their accuracy, yielding an estimator that always outperforms the empirical mean. Zhu et al. [60] arrived at an equivalent estimator to [4] from the self-training perspective within semi-supervised learning. Our primary benchmarks are PPI and PPI++; like these methods, we construct a correction term to de-bias ML predictions, but our approach provides a more fine-grained adjustment.

Several papers have since followed which improve the practical use of PPI-style estimators. While earlier work assumes access to a pre-trained ML model, Zrnic and Candès [62] uses cross-validation techniques to train the ML model from scratch utilizing the small labeled set of data. Zrnic [61] integrates the bootstrap method to prediction powered inference to facilitate applications where the central limit theorem justifications may be tenuous. While we assume access to a pre-trained model in this work, we remark that both cross-validation and bootstrap methods can be applied to our estimator using a formula similar to the previous papers.

Learning-Augmented Algorithms. Learning-augmented (LA) algorithms seek to enhance classical algorithms by incorporating the predictions of ML models trained on historical data. The framework has been successfully applied to many settings such as facility location [2, 6], mechanism design [8, 28], and scheduling problems [7, 24], among many others¹. To adapt the original framework of Lykouris and Vassilvitskii [37] to our setting, LA algorithms for mean estimation should output a confidence interval that 1) is tighter than the empirical mean when the predictions are accurate (*consistency*) and 2) retains the correct coverage probability when the predictions are arbitrarily poor (*robustness*). Similarly to [4, 5], we characterize the asymptotic distribution of the PART estimator, allowing us to build confidence intervals that satisfy both consistency and robustness.

Decision Tree for Mean Estimation. Decision trees have a long history, beginning with their use in exploratory data analysis by Morgan and Sonquist [41]. Breiman et al. [13] formalized modern regression trees for estimating conditional means with the CART algorithm. Subsequent work has extended and strengthened CART, e.g., unbiased-splitting methods [36] and popular ensemble approaches including “bagging” [11] and random forests [12]. We contribute to this line of literature by adapting the CART node splitting criteria of [13] to build the PART decision tree for mean residual estimation.

Monte Carlo Methods for Numerical Integration. A complementary line of work studies replacing empirical averages with carefully weighted sums to accelerate the convergence of integral estimates. It is well-known that integral of function on the unit interval can

¹See [1] for a up-to-date list of learning-augmented papers.

be approximated via an empirical average at a convergence rate of $O(n^{-1/2})$. Yakowitz et al. [58] was first to show that, for twice-differentiable functions on the unit interval, the canonical $O(n^{-1})$ rate can be improved to $O(n^{-4})$ via quadrature methods. Many results (e.g., [29, 46]) have since followed that observe convergence improvements through weighted sums. We adapt these quadrature methods to estimate the de-biasing term in our semi-supervised setting where the data is not uniformly distributed on the unit interval.

2 Preliminaries

In this section, we introduce the statistical framework that we use to present our result. We review the properties of empirical estimators, convergence concepts, and the central limit theorem. We also outline our modeling assumptions and define the core estimation problems, i.e., mean estimation and linear regression, that is the focus of our study.

Empirical Expectation and Variance. Let $\{Z_i\}_{i=1}^n$ be a sequence of independently and identically distributed random variables (i.i.d.) with mean $\mu = \mathbb{E}[Z]$ and variance $\sigma^2 = \text{Var}[Z] = \mathbb{E}[(Z - \mu)^2]$. The *empirical mean* is defined as $\hat{\mu}_n = \frac{1}{n} \sum_{i=1}^n Z_i$, and the *empirical variance* is defined as $\hat{\sigma}_n^2 = \frac{1}{n-1} \sum_{i=1}^n (Z_i - \hat{\mu}_n)^2$. It is easy to see that $\mathbb{E}[\hat{\mu}_n] = \mu$ and $\mathbb{E}[\hat{\sigma}_n^2] = \sigma^2$, i.e., $\hat{\mu}_n$ and $\hat{\sigma}_n^2$ are *unbiased* estimators of the mean and variance respectively.

Convergence in Distribution. A sequence of random variables $\{Z_n\}_{n=1}^\infty$ is said to converge in distribution to a random variable Y (denoted by $Z_n \xrightarrow{d} Y$) if, for every real number x at which the *cumulative distribution function* (CDF) $F_Y(x)$ is continuous, the CDF $F_{Z_n}(x)$ satisfies $\lim_{n \rightarrow \infty} F_{Z_n}(x) = F_Y(x)$.

Central Limit Theorem (CLT) and Confidence Intervals. The Central Limit Theorem states that for i.i.d. random variables $\{Z_i\}_{i=1}^n$ with finite variance σ^2 , the normalized empirical mean converges in distribution to a normal distribution, meaning that

$$\sqrt{n}(\hat{\mu}_n - \mu) \xrightarrow{d} \mathcal{N}(0, \sigma^2).$$

2.1 Model

In this work, we consider a dataset that includes two sets of data observations: *labeled* and *unlabeled* observations.

- The *labeled dataset* \mathcal{L} consists of n independent samples $\{(x_i, y_i)\}_{i=1}^n$ drawn from the joint distribution $P_{X,Y}$. Here, $x_i \in \mathcal{X} \subseteq \mathbb{R}^d$ is a d -dimensional feature vector, and $y_i \in \mathbb{R}$ is the corresponding outcome.
- The *unlabeled dataset* \mathcal{U} contains N feature vectors $\{\tilde{x}_j\}_{j=1}^N$ drawn from P_X which is the marginal distribution on X of $P_{X,Y}$. We assume that $N \gg n$, reflecting the practical scenario where unlabeled feature vectors are considerably easier to obtain than labels.

We further assume access to a machine learning predictor $f : \mathcal{X} \rightarrow \mathbb{R}$ that produces predicted outcomes for given feature vectors. Finally, for any $x \in \mathbb{R}^d$, we denote the k -th coordinate by $x^{(k)}$ for $k = 1, \dots, d$.

Mean Estimation and Linear Regression. In this work, we address two fundamental estimation problems: mean estimation and linear regression. For mean estimation, our objective is to accurately recover the expected value of the response, $\mu_Y = \mathbb{E}[Y]$, from the observed data. In the linear regression setting, we seek a linear model that minimizes the expected squared prediction error. Formally, we aim to find a parameter vector $\theta^* \in \mathbb{R}^d$ such that

$$\theta^* \in \arg \min_{\theta \in \mathbb{R}^d} \mathbb{E} \left[(Y - \theta^\top X)^2 \right],$$

where $X \in \mathbb{R}^d$ denotes the feature vector. These problems underpin our development of semi-supervised estimators that leverage both labeled and abundant unlabeled data to enhance estimation accuracy.

2.2 PPI & PPI++: The Case for the Mean

We review several competing approaches for prediction-powered inference in mean estimation, highlighting the key insights and underlying intuition behind each method.

Empirical Estimator. A common estimation problem is to estimate the mean outcome $\mu = \mathbb{E}[y]$ based on the labeled data. The classical empirical estimator is given by $\hat{\mu}_E = \frac{1}{n} \sum_{i=1}^n y_i$, which, via the CLT, satisfies

$$\sqrt{n}(\hat{\mu}_E - \mu) \xrightarrow{d} \mathcal{N}(0, \text{Var}(Y)).$$

PPI Estimator. Building on this approach, the PPI estimator, by Angelopoulos et al. [4], integrates the predictive model $f(x)$ with the unlabeled data. It is defined as

$$\hat{\mu}_{\text{PPI}} = \frac{1}{N} \sum_{j=1}^N f(\tilde{x}_j) + \frac{1}{n} \sum_{i=1}^n [y_i - f(x_i)].$$

The first term leverages predictions on the large unlabeled dataset, while the second term corrects for residual errors observed in the labeled data. Applying the CLT, the PPI estimator satisfies

$$\sqrt{n}(\hat{\mu}_{\text{PPI}} - \mu) \xrightarrow{d} \mathcal{N}(0, \text{Var}(Y - f(X))).$$

Assuming that $N \gg n$ and that the predictor $f(x)$ is sufficiently accurate (i.e., $\text{Var}(Y - f(X)) < \text{Var}(Y)$), the PPI estimator yields a narrower confidence interval for μ than the empirical estimator while preserving the same coverage probability.

PPI++ Estimator. In follow up work, Angelopoulos et al. [5] introduced a tuneable version of PPI defined by

$$\widehat{\mu}_{\text{PPI++}} = \frac{1}{N} \sum_{j=1}^N \widehat{\lambda} \cdot f(\tilde{x}_j) + \frac{1}{n} \sum_{i=1}^n \left[y_i - \widehat{\lambda} \cdot f(x_i) \right],$$

where $\widehat{\lambda} = \frac{\text{Cov}_n(Y, f(X))}{(1+n/N)\text{Var}_{n+N}(f(X_i))}$. Like PPI, this estimator remains unbiased. Applying the CLT, the PPI++ estimator satisfies

$$\sqrt{n}(\widehat{\mu}_{\text{PPI++}} - \mu) \xrightarrow{d} \mathcal{N}(0, \text{Var}(Y - \lambda \cdot f(X))),$$

where $\lambda = \frac{\text{Cov}(Y, f(X))}{(1+r)\text{Var}(f(X))}$ and $n/N \rightarrow r$. Unlike PPI, it is straightforward to show that this method produces confidence intervals that are at least as small as the empirical estimator. In particular, λ is the OLS coefficient between Y and f and therefore satisfies that $\text{Var}(Y - \lambda \cdot f(X)) \leq \text{Var}(Y)$.

3 Motivating Example:

A Static Partitioning Estimator for the Mean

Recall from [Section 2](#) that the PPI estimator provides an unbiased estimate of $\mu = \mathbb{E}[Y]$ by combining a large unlabeled dataset $\mathcal{U} = \{\tilde{x}_j\}_{j=1}^N$ with a labeled set $\mathcal{L} = \{(x_i, y_i)\}_{i=1}^n$. We remind that given a predictor $f : \mathcal{X} \rightarrow \mathbb{R}$, the PPI estimator is

$$\widehat{\mu}_{\text{PPI}} = \frac{1}{N} \sum_{j=1}^N f(\tilde{x}_j) + \frac{1}{n} \sum_{i=1}^n (y_i - f(x_i)).$$

While $\widehat{\mu}_{\text{PPI}}$ is unbiased and typically achieves variance lower than that of the simple empirical mean $\widehat{\mu}_E = \frac{1}{n} \sum_{i=1}^n y_i$, it relies on a *single, global residual correction* term $\frac{1}{n} \sum_{i=1}^n (y_i - f(x_i))$. In many applications, the distribution of residuals $(y - f(x))$ may vary significantly with certain key features in \mathcal{X} . Consequently, applying one global correction can leave some variability unexplained.

To illustrate how feature-specific corrections can reduce variance further, suppose there is a single feature (or coordinate) in \mathcal{X} that strongly influences the outcome Y . For concreteness, let X be a binary feature taking values in $\{-1, 1\}$. We define a *coordinate-partition estimator* that applies *group-specific* corrections for each partition $x \in \{-1, 1\}$ in [Estimator 1](#).

Estimator 1 (Coordinate-Partition Estimator). *Given a binary feature $X \in \{-1, 1\}$, define*

$$\widehat{p}_x = \frac{|\{i \in [1, \dots, N] : x_i = x\}|}{N}, \quad n_x = |\{i \in [1, \dots, n] : x_i = x\}|,$$

and let the group-specific average residual be

$$\widehat{r}_x = \frac{1}{n_x} \sum_{i:x_i=x} (y_i - f(x_i)).$$

Then the coordinate-partition estimator is

$$\hat{\mu}_C = \underbrace{\frac{1}{N} \sum_{j=1}^N f(\tilde{x}_j)}_{\text{predictive term}} + \underbrace{\sum_{x \in \{-1, 1\}} \hat{p}_x \hat{r}_x}_{\text{group-specific residual correction}}.$$

As shown in [Lemma 1](#), [Estimator 1](#) remains unbiased for μ and, as noted in [Corollary 2](#), it consistently attains weakly lower variance than the standard PPI estimator. We defer the proof of [Lemma 1](#) to [Section B](#).

Lemma 1 (Properties of [Estimator 1](#)). *Let $\hat{\mu}_C$ be the estimate from [Estimator 1](#), and assume $N \gg n$. Then $\hat{\mu}_C$ is an unbiased estimator for the mean $\mu = \mathbb{E}[Y]$. Moreover, when $\text{Var}(Y - f(X))$ is finite, and as $n \rightarrow \infty$,*

$$\sqrt{n} (\hat{\mu}_C - \mu) \xrightarrow{d} \mathcal{N}(0, \sigma_C^2), \text{ where } \sigma_C^2 := \sum_{x \in \{-1, 1\}} \Pr[X = x] \cdot \text{Var}(Y - f(X) \mid X = x).$$

Corollary 2 (Weak Variance Reduction). *Under the assumptions of [Lemma 1](#), the variance of [Estimator 1](#) $\hat{\mu}_C$ is at most that of the standard PPI estimator $\hat{\mu}_{\text{PPI}}$, e.g. $\text{Var}(\hat{\mu}_C) \leq \text{Var}(\hat{\mu}_{\text{PPI}})$.*

Sketch of Proof. Applying the law of total variance to the (binary) partitioned estimator $\hat{\mu}_C$ shows that it can be expressed as a weighted sum of group-specific residuals and a non-negative term. \square

In [Example 1](#) below, we also show that by capturing heterogeneous behavior in the conditional residual $y - f(x)$, the estimator can achieve a strict variance reduction in settings where the residual variability differs substantially across partitions.

Example 1 (Strict Variance Reduction). *Consider a binary feature X taking values in $\{-1, 1\}$ with probability $1/2$ each. Conditional on X , let $Y - f(X)$ be normally distributed:*

$$Y - f(X) \mid (X = 1) \sim \mathcal{N}(1, 1), \quad Y - f(X) \mid (X = -1) \sim \mathcal{N}(-1, 1).$$

Hence, $\mathbb{E}[Y - f(X)] = 0$. Suppose we estimate μ via:

- **PPI estimator**, μ_{PPI} , which applies one global residual correction.
- **Coordinate-partition estimator**, μ_C , which corrects separately for $X = 1$ and $X = -1$.

Straightforward variance calculation shows: $\text{Var}(\mu_{\text{PPI}}) = \frac{2}{n} > \text{Var}(\mu_C) = \frac{1}{n}$.

In summary, while both the standard PPI estimator and the conditional estimator are unbiased for the true mean μ , conditioning on X reduces the variance from approximately $\frac{2}{n}$ to $\frac{1}{n}$. This variance reduction illustrates the potential gains from incorporating feature information. Our proposed PART Estimator generalizes this idea by adaptively partitioning the feature space into regions of approximately homogeneous residual variance, thereby leveraging both labeled and unlabeled data to obtain more efficient confidence intervals without sacrificing unbiasedness.

4 The PART Estimator:

An Adaptive Partitioning Estimator

In this section, we describe the PART estimator and discuss its application to building confidence intervals for the mean and linear regression coefficients. At a high-level, the PART estimator uses a CART-style binary tree to partition the feature space with splits chosen to minimize the variance of the debiasing term greedily. Inside each leaf of the tree, we compute a local residual correction using nearby labeled points. We then take a mixture of these local corrections based on the fraction of unlabeled data assigned to each leaf to produce the overall debiasing term. We highlight that when we set the depth of the PART tree equal to zero, we recover the PPI estimator; this guarantees that with appropriate depth-parameter tuning PART will perform at least as well as PPI. In forthcoming sections we will establish the asymptotic properties of the PART estimator and prove coverage guarantees.

4.1 Estimating the Mean

Recall that our feature space is $\mathcal{X} \subset \mathbb{R}^d$ and that we denote the set of unlabeled observations by $\mathcal{U} = \{\tilde{x}_i\}_{i=1}^N$ and the set of labeled observations by $\mathcal{L} = \{(x_i, y_i)\}_{i=1}^n$. The predictor is given by $f : \mathcal{X} \rightarrow \mathbb{R}$, and for each labeled observation (x_i, y_i) the residual is defined as $r(x_i, y_i) := y_i - f(x_i)$. Our objective is to partition the feature space \mathcal{X} into subregions that exhibit low residual variance by constructing a binary decision tree T .

Assumption 1. *We assume $N \gg n$, i.e., the number of unlabeled observations is significantly larger than the number of labeled ones. For simplicity in our analysis, we also assume that we have direct access to the mass function $p(\mathcal{R})$ for any candidate subregion $\mathcal{R} \subseteq \mathcal{X}$, e.g. $p(\mathcal{R}) = \Pr[X \in \mathcal{R}]$.*

We remark that this assumption is well-supported if $N \gg n$. Namely, any candidate sub-region $\mathcal{R} \subset \mathcal{X}$ produced by PART must be formed by axis-aligned hyperplanes. It is well-known (e.g., [40]) that the VC dimension of axis-aligned rectangles in \mathbb{R}^d is $O(d)$. If we let $\hat{p}_N(\mathcal{R}) = \frac{1}{N} \sum_{i=j}^N \mathbf{1}\{\tilde{x}_j \in \mathcal{R}\}$, then by standard uniform convergence arguments (e.g. Corollary 3.19 of [40]), we can show that for some absolute constant C and any $\delta \in (0, 1)$, it holds that

$$|\hat{p}_N(\mathcal{R}) - p(\mathcal{R})| \leq C \cdot \sqrt{\frac{d \log(N/d) + \log(1/\delta)}{N}}.$$

Under the assumption that $N \gg n$, it follows that $|\hat{p}_N(\mathcal{R}) - p(\mathcal{R})| = o(n^{-1/2})$ and therefore this term can be safely ignored in our asymptotic analysis.

Candidate Splitting Points. At each internal node corresponding to a region $\mathcal{R} \subseteq \mathcal{X}$, a feature coordinate $k \in \{1, \dots, d\}$ is selected for splitting. Concretely, let $\{\tilde{x}_i^{(k)} : \tilde{x}_i \in \mathcal{U}\}$ denote the collection of k -th coordinate values from the unlabeled observations. We then compute the empirical quantiles $q_1^{(k)}, q_2^{(k)}, \dots, q_n^{(k)}$ at levels $\frac{1}{n}, \frac{2}{n}, \dots, \frac{n-1}{n}$, where n is the total number of labeled observations.

Rather than employing these quantile values directly as splitting thresholds, we define the set of candidate splitting points as the midpoints between consecutive quantiles:

$$\mathcal{S}^{(k)} := \left\{ \frac{q_j^{(k)} + q_{j+1}^{(k)}}{2} : j = 1, 2, \dots, n-2 \right\}.$$

Remark 1. *This candidate splitting strategy is analogous to conventional tree-splitting methods that utilize midpoints between sorted input values. We adopt this standard approach because it leads to less variability in the splitting points, which in turn simplifies the derivation of confidence intervals for the final estimator.*

Splitting Function. Let $\mathcal{R} \subseteq \mathcal{X}$ denote the region corresponding to an internal node of the tree. For a candidate splitting coordinate $k \in \{1, \dots, d\}$ and a candidate threshold $s^{(k)}$ chosen from the set $\mathcal{S}^{(k)}$, we partition \mathcal{R} into two disjoint subregions:

$$\mathcal{R}_{\text{left}} = \{x \in \mathcal{R} : x^{(k)} \leq s^{(k)}\}, \quad \mathcal{R}_{\text{right}} = \{x \in \mathcal{R} : x^{(k)} > s^{(k)}\}.$$

Define the sets of labeled observations in the two regions as

$$\mathcal{L}_{\text{left}} = \{(x_i, y_i) \in \mathcal{L} : x_i \in \mathcal{R}_{\text{left}}\} \quad \text{and} \quad \mathcal{L}_{\text{right}} = \{(x_i, y_i) \in \mathcal{L} : x_i \in \mathcal{R}_{\text{right}}\}.$$

Let $n_{\text{left}} = |\mathcal{L}_{\text{left}}|$, $n_{\text{right}} = |\mathcal{L}_{\text{right}}|$ denote the number of labeled observations in the respective regions. Similarly, define the proportions of unlabeled observations in the two regions as $p_{\text{left}} = p(X \in \mathcal{R}_{\text{left}})$, and $p_{\text{right}} = p(X \in \mathcal{R}_{\text{right}})$.²

For each child region, we define the sample variance of the residuals over the corresponding labeled data. In particular, for the left child region, let

$$\hat{\sigma}_{\text{left}}^2 = \frac{1}{n_{\text{left}} - 1} \sum_{(x,y) \in \mathcal{L}_{\text{left}}} \left(r(x, y) - \bar{r}_{\text{left}} \right)^2,$$

and analogously, define

$$\hat{\sigma}_{\text{right}}^2 = \frac{1}{n_{\text{right}} - 1} \sum_{(x,y) \in \mathcal{L}_{\text{right}}} \left(r(x, y) - \bar{r}_{\text{right}} \right)^2,$$

where \bar{r}_{left} (respectively, \bar{r}_{right}) is the mean residual computed over $\mathcal{L}_{\text{left}}$ (respectively, $\mathcal{L}_{\text{right}}$).

We then define the *Variance of Mixture of Splits* (VMS) criterion for the candidate split (k, s) as

$$\text{VMS}(k, s, \mathcal{R}) := p_{\text{left}}^2 \frac{\hat{\sigma}_{\text{left}}^2}{n_{\text{left}}} + p_{\text{right}}^2 \frac{\hat{\sigma}_{\text{right}}^2}{n_{\text{right}}}.$$

The optimal split at the node is chosen as the candidate (k^*, s^*) that minimizes the VMS criterion, i.e.,

$$(k^*, s^*) = \arg \min_{(k,s): k \in \{1, \dots, d\}, s \in \mathcal{S}^{(k)}} \text{VMS}(k, s, \mathcal{R}).$$

²We remind that these quantities can be estimated via the unlabeled samples \mathcal{U} -see [Assumption 1](#).

Remark 2. The VMS criterion quantifies the variance reduction from splitting the region \mathcal{R} . By leveraging the abundant unlabeled data, we obtain highly accurate estimates of the mass in each subregion— p_{left} and p_{right} . Consequently, minimizing the VMS criterion favors splits that not only create groups with more homogeneous residuals but also benefit from mass estimates from the unlabeled data with negligible variance.

Termination Criterion. The recursive splitting is halted when either the tree reaches a predetermined maximum depth D or when the number of labeled observations within a region drops below a specified minimum threshold m . At termination, the feature space is partitioned into L leaf regions, denoted by $\{\mathcal{R}_\ell\}_{\ell=1}^L$. For each leaf region \mathcal{R}_ℓ , we calculate:

1. The average residual $\bar{r}_\ell := \frac{1}{n_\ell} \sum_{(x_i, y_i) : x_i \in \mathcal{R}_\ell} r(x_i, y_i)$, where $n_\ell = |\{(x_i, y_i) : x_i \in \mathcal{R}_\ell\}|$ is the number of labeled observations in \mathcal{R}_ℓ .
2. The proportion of unlabeled observations $p_\ell = p(\mathcal{R}_\ell)$. Recall that this quantity can be estimated from the unlabeled data—see [Assumption 1](#).

Using these quantities, the final population mean estimator is defined as:

$$\hat{\mu}_T := \frac{1}{N} \sum_{i=1}^N f(\tilde{x}_i) + \sum_{\ell=1}^L p_\ell \bar{r}_\ell.$$

The pseudo-code of this estimator is presented in [Algorithm 1](#) in [Section A](#).

4.1.1 Constructing Confidence Intervals

We form confidence intervals by estimating the variance of $\hat{\mu}_T$ using empirical residual variances in each leaf region, yielding a Wald-type interval [\[54\]](#) with asymptotically valid coverage. For each leaf \mathcal{R}_ℓ , let

$$\hat{\sigma}_\ell^2 := \frac{1}{n_\ell - 1} \sum_{\substack{(x_i, y_i) \in \mathcal{L}: \\ x_i \in \mathcal{R}_\ell}} (r(x_i, y_i) - \bar{r}_\ell)^2,$$

be the variance of the residuals of labeled data in $\mathcal{L} \cap \mathcal{R}_\ell$. We estimate the variance of $\hat{\mu}_T$ by $\hat{\sigma}^2 := \sum_{\ell=1}^L p_\ell^2 \frac{\hat{\sigma}_\ell^2}{n_\ell}$, yielding the Wald-type $(1 - \alpha)$ confidence interval

$$\left[\hat{\mu}_T - z_{1-\alpha/2} \hat{\sigma}, \hat{\mu}_T + z_{1-\alpha/2} \hat{\sigma} \right],$$

where $z_{1-\alpha/2}$ is the $(1 - \alpha/2)$ standard normal quantile. We formally show coverage probabilities in [Theorem 1](#). The proof is postponed to [Section C](#).

Theorem 1 (Coverage of [Algorithm 1](#)). *Fix level $\alpha \in (0, 1)$. Let $\{(x_i, y_i)\}_{i=1}^n$ be i.i.d. samples drawn from the joint distribution $P_{X,Y}$ and $\{\tilde{x}_j\}_{j=1}^N$ be i.i.d. samples drawn from the marginal P_X . Then, under [Assumption 1](#) and as $n \rightarrow \infty$, the output of [Algorithm 1](#)—restricted to at most L leaf nodes—satisfies:*

$$\Pr \left[\mu \in \left[\hat{\mu}_T - z_{1-\alpha/2} \hat{\sigma}, \hat{\mu}_T + z_{1-\alpha/2} \hat{\sigma} \right] \right] \geq 1 - \alpha - \sqrt{\frac{2L \cdot \log(d \cdot n)}{n}} - \frac{1}{(n \cdot d)^L}.$$

Remark 3. [Theorem 1](#) highlights that the nominal coverage level of $1 - \alpha$ is adjusted downward by terms that quantify finite-sample effects. Notably, the term

$$\sqrt{\frac{2L \cdot \log(d \cdot n)}{n}}$$

is dominant this adjustment. As the number of allowed leaf nodes L increases, the model becomes more complex, which in turn amplifies the implicit correction term. Consequently, while the asymptotic guarantee might suggest nominal coverage, in practice the confidence intervals are narrower than expected due to overfitting, thereby reducing their true coverage probability. This insight underscores the trade-off between model flexibility and the reliability of statistical inference.

We now examine how the finite-sample correction term in [Theorem 1](#) manifests empirically. [Figure 1](#) compares [Theorem 1](#)'s theoretical coverage bound (dashed lines) with the realized coverage probability of the PART estimator (solid lines). The figure demonstrates that PART substantially outperforms the theoretical bounds in practice, achieving a coverage close to the desired 95% confidence level.

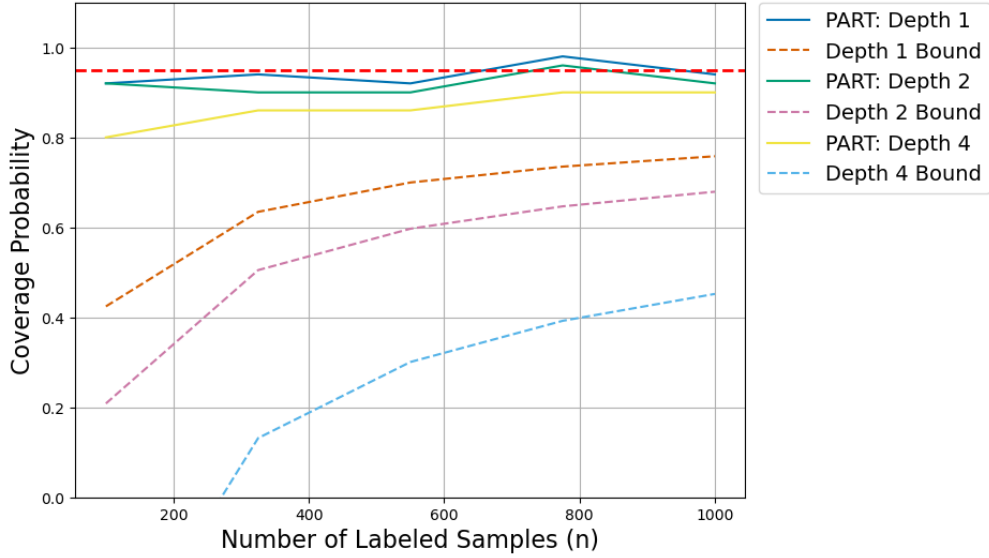


Figure 1: Theoretical coverage of [Theorem 1](#) (dashed lines) versus empirical coverage for the PART estimator (solid lines) at a 95% confidence level.

4.2 Estimating Linear Regression Coefficients

We now adapt the PART estimator to construct narrow confidence intervals for regression coefficients by adaptively partitioning the feature space. Our focus is on estimating the k th component of the correction vector, $\theta^{(k)}$, in the linear regression model.

Let \tilde{X} be the unlabeled design matrix with rows \tilde{x} drawn from \mathcal{U} . Define the predictor-augmented estimator as $\tilde{\theta} = \tilde{X}^+ f(\tilde{X})$, where \tilde{X}^+ is the Moore–Penrose pseudoinverse and $f(\tilde{X})$ is the vector of predictor function values. Our goal is to debias $\tilde{\theta}$.

Assuming that the number of unlabeled observations N is much larger than the number of labeled observations n (i.e., $N \gg n$), the law of large numbers implies $\tilde{\Sigma} = \frac{1}{N} \sum_{i=1}^N \tilde{x}_i \tilde{x}_i^T \rightarrow \mathbb{E}[xx^T]$, so that $\tilde{\theta} \approx (\mathbb{E}[xx^T])^{-1} \mathbb{E}[xf(x)]$. Under the standard linear model, the true parameter is given by

$$\theta = (\mathbb{E}[xx^T])^{-1} \mathbb{E}[xy].$$

We extend the approach in Section 4.1 to linear regression by modifying the splitting rule and variance estimation to rigorously account for the uncertainty in $\theta^{(k)}$ while preserving the candidate splitting points.

Notation and Preliminaries. For any subregion $\mathcal{R} \subseteq \mathcal{X}$, define $\mathcal{L}_{\mathcal{R}} = \{(x_i, y_i) \in \mathcal{L} : x_i \in \mathcal{R}\}$, with sample size $n_{\mathcal{R}} = |\mathcal{L}_{\mathcal{R}}|$ and probability $p_{\mathcal{R}} = \Pr(x \in \mathcal{R})$. Let $X_{\mathcal{R}}$ and $Y_{\mathcal{R}}$ denote the features and responses in \mathcal{R} , respectively. We define the residual vector by

$$\hat{R}_{\mathcal{R}} = \frac{1}{n_{\mathcal{R}}} \tilde{\Sigma}^{-1} X_{\mathcal{R}}^T (Y_{\mathcal{R}} - f(X_{\mathcal{R}})).$$

For variance estimation, define the bias term as

$$\hat{M}_{\mathcal{R}} = \widehat{\text{Cov}}(X_{\mathcal{R}}^T (Y_{\mathcal{R}} - f(X_{\mathcal{R}}))) = \frac{1}{n_{\mathcal{R}} - 1} \sum_{(x,y) \in \mathcal{L}_{\mathcal{R}}} \left(y - f(x) - x^T \hat{R}_{\mathcal{R}} \right)^2 xx^T,$$

and set

$$\hat{V}_{\mathcal{R}} = \tilde{\Sigma}^{-1} \hat{M}_{\mathcal{R}} \tilde{\Sigma}^{-1}.$$

We further make the following assumption to use the high-dimensional central limit theorem.

Assumption 2. For any $\mathcal{R} \subseteq \mathcal{X}$, the matrix $\text{Cov}[x(f(x) - y) \mid x \in \mathcal{R}]$ is invertible and $p_{\mathcal{R}} > 0$.

This is standard non-degeneracy assumption used for inference on generalized linear models (GLM) in high-dimensional settings, which we have adapted to hold on a leaf-by-leaf basis (see, e.g., [5, 54]). [Assumption 2](#) guarantees that for each leaf, the covariance of the score function is invertible, which means that the asymptotic variance of the region $V_{\mathcal{R}}$ is well-defined.

We defer the proof of the asymptotic distribution of the residual vector $\hat{R}_{\mathcal{R}}$ ([Theorem 2](#)) to [Section D](#).

Theorem 2. Define $V_{\mathcal{R}} = \tilde{\Sigma}^{-1} \text{Var}[x(f(x) - y) \mid x \in \mathcal{R}] \tilde{\Sigma}^{-1}$. Under [Assumption 2](#), as $n \rightarrow \infty$,

$$\hat{R}_{\mathcal{R}} \xrightarrow{d} \mathcal{N}\left((\mathbb{E}[xx^T])^{-1} \mathbb{E}[x(y - f(x)) \mid x \in \mathcal{R}], \frac{V_{\mathcal{R}}}{n_{\mathcal{R}}} \right),$$

and $\hat{V}_{\mathcal{R}}$ is a consistent estimator of $V_{\mathcal{R}}$.

Splitting Function for Linear Regression. To enhance the precision in estimating $\theta^{(k)}$, we partition the feature space adaptively. Let $\mathcal{R} \subseteq \mathcal{X}$ be a region corresponding to an internal node in the tree. For each candidate splitting feature coordinate $j \in \{1, \dots, d\}$ and candidate threshold $s^{(j)}$, chosen from a pre-specified set $\mathcal{S}^{(j)}$, (see [Section 4.1](#)) we partition \mathcal{R} into two disjoint subregions $\mathcal{R}_{\text{left}} = \{x \in \mathcal{R} : x^{(j)} \leq s^{(j)}\}$, $\mathcal{R}_{\text{right}} = \{x \in \mathcal{R} : x^{(j)} > s^{(j)}\}$.

To get unbiased estimation of the k th coefficient with lower variance, we use the k th diagonal element of the covariance matrices, $\widehat{V}_{\mathcal{R}_{\text{left}}}^{(k,k)}, \widehat{V}_{\mathcal{R}_{\text{right}}}^{(k,k)}$ and we define the *Variance of Mixture of Splits for Linear Regression* (VMS_{LR}) criterion for the candidate split $(j, s^{(j)})$ as

$$\text{VMS}_{\text{LR}}(j, s^{(j)}, \mathcal{R}) := p_{\mathcal{R}_{\text{left}}}^2 \frac{\widehat{V}_{\mathcal{R}_{\text{left}}}^{(k,k)}}{n_{\text{left}}} + p_{\mathcal{R}_{\text{right}}}^2 \frac{\widehat{V}_{\mathcal{R}_{\text{right}}}^{(k,k)}}{n_{\text{right}}}.$$

The candidate split that minimizes this criterion is selected:

$$(j^*, s^{(j^*)}) = \arg \min_{\substack{j \in \{1, \dots, d\} \\ s^{(j)} \in \mathcal{S}^{(j)}}} \text{VMS}_{\text{LR}}(j, s^{(j)}, \mathcal{R}).$$

This choice of splitting aims to create subregions in which the uncertainty in estimating $\theta^{(k)}$ is minimized, thereby contributing to tighter overall confidence intervals.

Termination Criterion. We terminate the recursive splitting when either the tree reaches a predetermined maximum depth D or when the number of labeled observations in a region falls below a minimum threshold m . At termination, the feature space is partitioned into L leaf regions, denoted by $\{\mathcal{R}_\ell\}_{\ell=1}^L$. The final estimator for the k th coordinate is defined as

$$\widehat{\theta}_T^{(k)} := \widetilde{\theta}^{(k)} + \sum_{\ell=1}^L p_{\mathcal{R}_\ell} \widehat{R}_{\mathcal{R}_\ell}^{(k)}.$$

The pseudo-code of this estimator is presented in [Algorithm 2](#) in [Section A](#).

4.2.1 Constructing Confidence Intervals

We define the empirical variance estimator as $\widehat{\sigma}^2 = \sum_{\ell=1}^L p_{\mathcal{R}_\ell}^2 \frac{\widehat{V}_{\mathcal{R}_\ell}^{(k,k)}}{n_{\mathcal{R}_\ell}}$. Using this variance estimate, we construct a standard Wald-type [\[54\]](#) $1 - \alpha$ confidence interval for the k th coefficient:

$$\left[\widehat{\theta}_T^{(k)} - z_{1-\alpha/2} \widehat{\sigma}, \quad \widehat{\theta}_T^{(k)} + z_{1-\alpha/2} \widehat{\sigma} \right].$$

Theorem 3 (Asymptotic Coverage). *Assume that*

1. $\{(x_i, y_i)\}_{i=1}^n$ are i.i.d. from $P_{X,Y}$ and $\{\tilde{x}_j\}_{j=1}^N$ are i.i.d. from P_X with $N \gg n$,
2. the tree estimator uses a fixed number L of leaves,
3. [Assumption 2](#) holds.

Then, as $n \rightarrow \infty$,

$$\lim_{n \rightarrow \infty} \Pr \left[\theta^{(k)} \in \left[\widehat{\theta}_T^{(k)} - z_{1-\alpha/2} \widehat{\sigma}, \quad \widehat{\theta}_T^{(k)} + z_{1-\alpha/2} \widehat{\sigma} \right] \right] = 1 - \alpha.$$

Proof sketch. We prove that the estimator $\widehat{\theta}_T^{(k)}$ is unbiased for the regression coefficient $\theta^{(k)}$ and follows a normal distribution. Moreover, the variance estimator $\widehat{\sigma}^2$ is shown to be consistent for the true variance.

Observe that

$$\begin{aligned} \mathbb{E}[\widehat{\theta}_T^{(k)}] &= \left(\mathbb{E}[xx^T] \right)^{-1} \mathbb{E}[xf(x)] + \sum_{\ell=1}^L p_{\mathcal{R}_\ell} \mathbb{E}[\widehat{R}_{\mathcal{R}_\ell}^{(k)}] \\ &= \left(\mathbb{E}[xx^T] \right)^{-1} \mathbb{E}[xf(x)] + \sum_{\ell=1}^L p_{\mathcal{R}_\ell} \left(\mathbb{E}[xx^T] \right)^{-1} \mathbb{E}[x(y - f(x)) \mid x \in \mathcal{R}] \\ &= \left(\mathbb{E}[xx^T] \right)^{-1} \left(\mathbb{E}[xf(x)] + \sum_{\ell=1}^L \mathbb{E}[x(y - f(x)) \wedge x \in \mathcal{R}] \right) \\ &= \left(\mathbb{E}[xx^T] \right)^{-1} (\mathbb{E}[xf(x)] + \mathbb{E}[x(y - f(x))]) \\ &= \left(\mathbb{E}[xx^T] \right)^{-1} xy \\ &= \theta^{(k)}, \end{aligned}$$

where in the second equality we used [Theorem 2](#). The consistency of the variance estimator follows directly by [Theorem 2](#) and the fact that for two different leaves $\ell \neq \ell'$, $\text{Cov}[\widehat{R}_{\mathcal{R}_\ell}^{(k)}, \widehat{R}_{\mathcal{R}_{\ell'}}^{(k)}] = 0$.³ \square

5 Experimental Performance of PART

We test the experimental performance of PART estimator on a variety real-world datasets. We utilize PPI++ as the baseline and omit classical PPI, as PPI++ consistently outperforms PPI. In every experiments, we find that the PART estimator consistently delivers tighter confidence intervals compared to PPI++. In [Section 5.1](#), we demonstrate that increasing the depth of the tree beyond a depth of one can yield further improvements without overfitting.

Methodology. For our testing methodology, we assume that each dataset has M i.i.d. samples consisting of features, labels, and predicted labels. For various fixed values of n , we randomly obfuscate $N = M - n$ of the labels to produce N pieces of unlabeled data and n pieces of labeled data. We subsequently run the PART estimator using a manually tuned depth limit on the labeled and unlabeled data, recording the width of the confidence interval and whether the interval contained the true mean. We repeat the previous procedure 100 times for each fixed n and compute the average confidence interval width and the coverage probability. We produce two graphs to show how the width of the intervals and coverage probability changes as a function of n . For the interval width graph, we include one standard

³The proof follows similarly to [Claim 3](#).

deviation bars on each measured n value. We show the nominal coverage probability with a constant dashed grey line.

5.1 Predicting Mean Deforestation Rate from Satellite Imagery

Deforestation in the Amazon rainforest disrupts local ecosystems and releases stored carbon [14, 34]. This motivates the remote monitoring of forest cover through satellite imagery [48]. We seek to measure the mean deforestation rate in the forest cover data provided by [14] using the PART estimator. The dataset consists of 1596 observations with labels corresponding to whether deforestation in a particular tract of land is evident. We use predictions generated from a histogram-based gradient-boosted tree trained by [4]. Figure 2 demonstrates that trees with non-zero depth can result in smaller confidence intervals while still remaining valid.

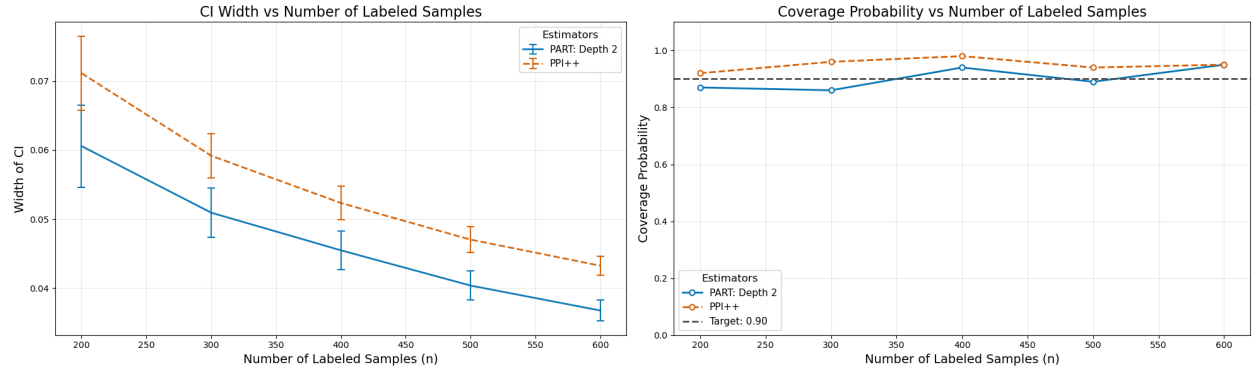


Figure 2: Estimating the mean deforestation rate in the Amazon rainforest from satellite imagery [14] (see Section 5 for testing methodology).

5.2 Estimating Mean Fraction of Spiral Galaxies

The Galaxy Zoo 2 project [56] is an crowd-sourced initiative focused on providing morphological classifications for 304,122 galaxies captured by the Sloan Digital Sky Survey [59]. These human-annotated labels serve as key aids in helping scientists understand galaxy evolution (e.g., [18]) but require substantial manual effort. To mitigate this, machine learning approaches—such as the convolutional neural network of Dieleman et al. [22]—predict morphology directly from the images. In this experiment, we follow this trend by using an ML model to help estimate the mean fraction of spiral galaxies in the local universe (see Figure 3). Our dataset consists of 16,743 total observations where each label is the estimated probability that the galaxy is spiral. We use predictions from a ResNet50 model supplied by [4].

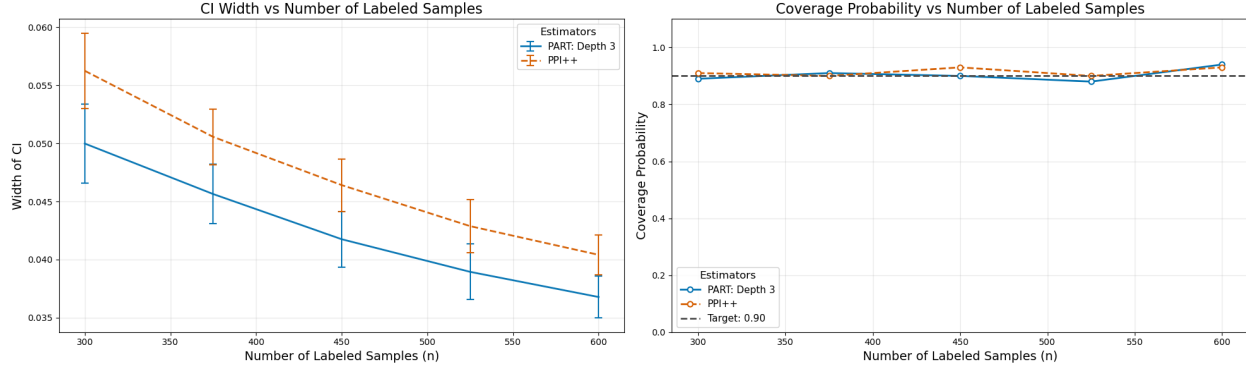


Figure 3: Estimating the mean fraction of spiral galaxies in the universe using Galaxy Zoo 2 data [56] (see Section 5 for testing methodology).

5.3 Measuring Mean Quality of Portuguese Wine

Vinho Verde wine originates from the Minho Province of Portugal, where it is tightly regulated under Denominação de Origem Controlada (DOC) system. To deter counterfeiting, regulators use physicochemical and sensory tests to assess wine quality. Cortez et al. [20] provide a dataset of 1280 wine samples, each with 11 features (pH, sulphates, alcohol content, etc) gathered via physicochemical tests and a quality score on a 0-10 scale. This dataset has become a standard benchmark for ensemble tree methods (e.g., [42]). Our objective is to estimate the average wine quality on this dataset using the PART estimator. For predictions, we train a Random Forest Classifier on 20% of the data and generate predicted scores for the remaining 80% of the data. We display the resulting confidence interval widths and coverage probabilities in Figure 4.

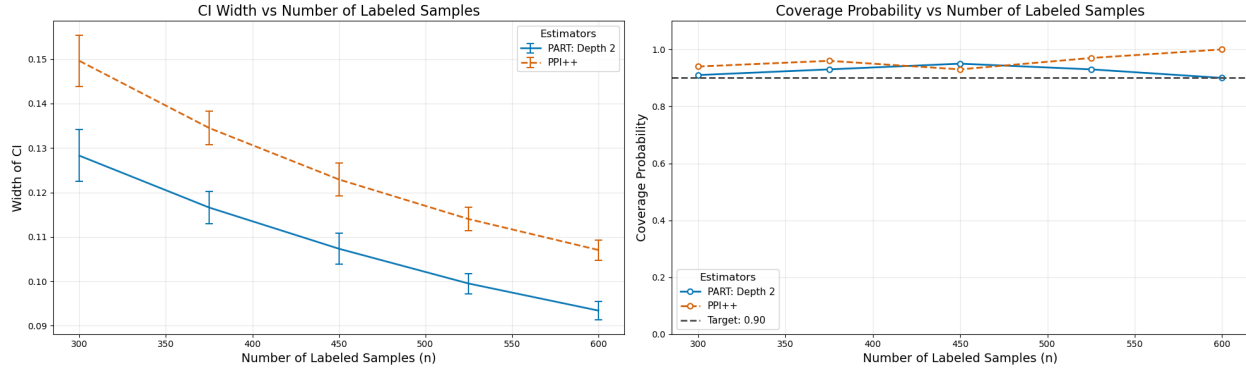


Figure 4: Estimating the mean quality of Portuguese Vinho Verde wine [20] (see Section 5 for testing methodology).

5.4 Estimating Average Median House Price using Census Data

California's housing market is shaped by many factors, including its coastal geography and strict zoning laws. One source of information about the housing market comes from census data. Pace and Barry [45] initially used the 1990 California Census to form a dataset

consisting of 16,512 instances with 9 characteristics (population, number of households, total rooms, etc.) and 1 outcome variable indicating the median house value in the block (a geographical unit used by the Census Bureau). Many textbooks (e.g., [26]) use this dataset as a standard ML benchmark. Our goal is to use this dataset to estimate the average median house price in a block group in California (see Figure 5 for results). For predictions, we train a Random Forest Regressor on 20% of the data and generate predicted scores for the remaining 80% of the data.

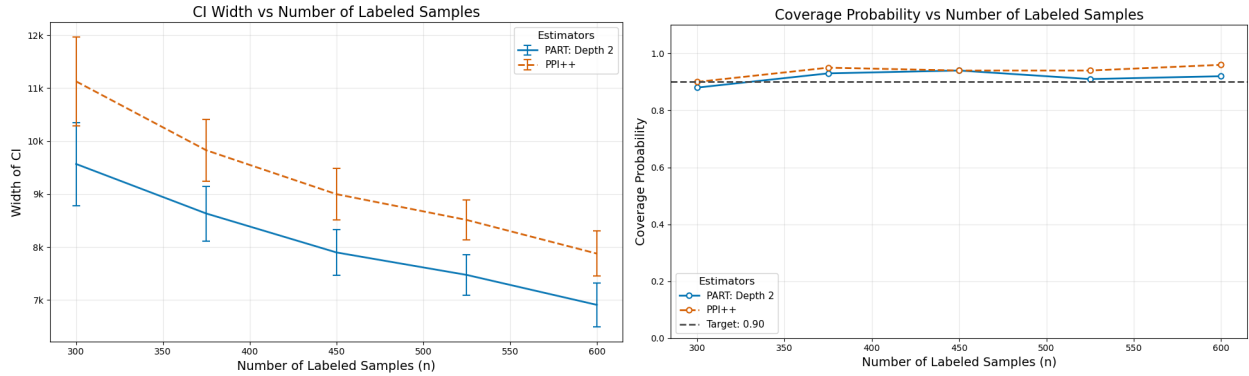


Figure 5: Estimating the average median house price in a census block using California census data [26] (see Section 5 for testing methodology).

5.5 Estimating Odds Ratio of Protein Structures via AlphaFold

Since the groundbreaking result of [31], AlphaFold has quickly become an essential tool used by researchers to allow the study of the structure of proteins on a mass scale (e.g., see [44, 52, 57] among many others). Predictions from AlphaFold were recently used by Bludau et al. [10] to understand whether intrinsically disordered regions (IDRs) on proteins experience phosphorylation at a greater rate. In this task, we use data from [53] consisting of 10,802 samples and apply it to the PART estimator with the goal of predicting the odds ratio for a protein being phosphorylated and belonging to an IDR (see Figure 6 for results).

⁴ We utilize the AlphaFold-based predictions from [4].

⁴ For the precise derivation of the confidence interval for the odds ratio, which requires use of the delta method, see [5].

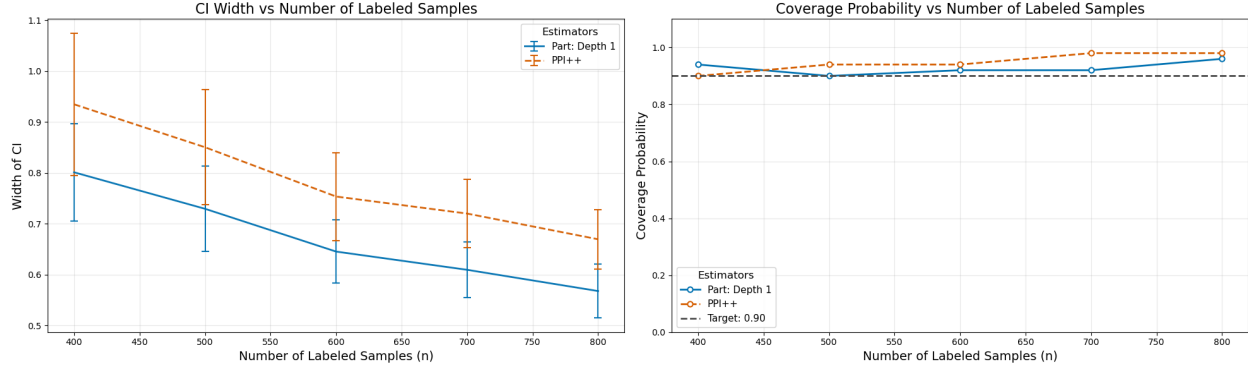


Figure 6: Estimating the odds ratio of a protein being phosphorylated and belonging to an intrinsically disordered region using AlphaFold predictions [53] (see Section 5 for testing methodology).

5.6 Estimating Linear Relationship between Income and Physical Characteristics on Census Data

A persistent correlation between sex and earnings is well documented in the economics literature [9]. We use census data from Ding et al. [23] to estimate a linear relationship between sex (M/F) and individual income. The dataset consists of 380,091 observations with two features, sex (M/F) and age (0-99), and a label for the person’s income. For predictions, we utilize an XGBoost model trained by [5]. We graph the confidence interval width and coverage probabilities in Figure 7.

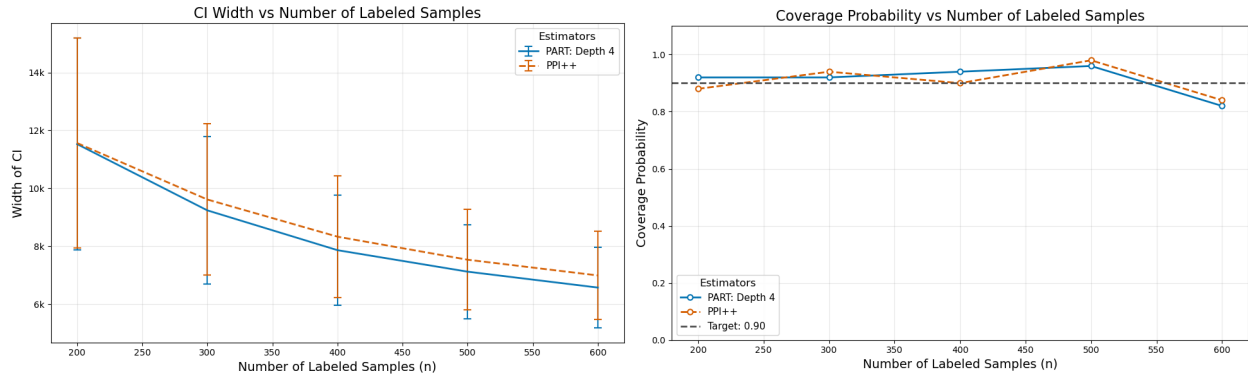


Figure 7: Estimating the linear regression coefficient between income and sex (M/F) on California census data [23] (see Section 5 for testing methodology).

6 The PAQ Estimator: *Exploring the Partitioning Limit*

In the previous sections, we built tree-based estimators that reduce variance by partitioning the feature space into homogeneous regions and computing local bias estimates for each

region. Like PPI and PPI++, the convergence rates of these estimators are still limited by the number of labeled points that fall into each region, which unavoidably forces a $O(n^{-1})$ convergence rate for the variance.

In this section, we analyze the PAQ estimator by examining the behavior of the PART estimator in the limiting scenario where the tree depth grows without bound. In particular, as the depth increases, the diameter of each leaf region shrinks until it eventually contains only two labeled points. Under the assumption that the residual function is deterministic and Lipschitz (see [Assumption 3](#)), we show that within these small regions, the debiasing term can be expressed as an integral over the feature space. This structure allows us to apply numerical quadrature techniques on the labeled data to approximate the integral efficiently. As a consequence, the PAQ estimator is able to circumvent the $O(n^{-1})$ convergence rate for the variance that traditionally appears in univariate mean estimation.

Henceforth, we focus on the regime in which the response variable is deterministic, and the residual function $r(x) = y(x) - f(x)$ is smooth (see [Assumption 3](#) below).

Assumption 3. *We assume that the residual function $r : \mathbb{R} \rightarrow \mathbb{R}$ is a deterministic, C^2 function satisfying that $\sup_x |r'(x)| \leq L_1$ and $\sup_x |r''(x)| \leq L_2$.*

As before, we assume that we have a small set of labeled data $\mathcal{L} = (x_i, y_i)_{i=1}^n$ drawn from a joint distribution $P_{X,Y}$ and a large set of unlabeled data $\mathcal{U} = (\tilde{x}_i)_{i=1}^N$ drawn from the marginal P_X . For each $\tilde{x}_i \in \mathcal{U}$, we define its nearest-neighbor in \mathcal{L} by

$$h(\tilde{x}_i) = \arg \min_{x \in \mathcal{L}} |\tilde{x}_i - x|.$$

The PAQ estimator then adjusts the model output $f(\tilde{x}_i)$ by the residual of its nearest labeled neighbor:

$$\mu_{PAQ} = \frac{1}{N} \sum_{i=1}^N f(\tilde{x}_i) + r(h(\tilde{x}_i)).$$

Intuitively, when r is smooth, $r(\tilde{x}_i) \approx r(h(\tilde{x}_i))$, the PAQ estimator utilizes more information than a plain average of $r(x_i)$. The key idea is to approximate the residual at an unlabeled point using the residual of its nearest labeled neighbor, thereby exploiting the smooth structure of the residual function without requiring explicit partitioning. In the following, we characterize the bias and variance of this estimator when the marginal P_X is a standard uniform distribution. We include a detailed proof of this theorem in [Section E](#).

Theorem 4 (PAQ Estimator, Degree-One Interpolation). *Under [Assumption 3](#) and $P_X = \mathcal{U}_{[0,1]}$, it holds that*

$$|\mathbb{E}[\mu_{PAQ}] - \mathbb{E}[Y]| = O\left(\frac{1}{n^2}\right) \quad \text{and} \quad \text{Var}(\mu_{PAQ}) = O\left(\frac{1}{N} + \frac{1}{n^4}\right).$$

High-Level Proof Overview. Observe that the $f(\tilde{X}_i)$ terms are i.i.d., so by the Central Limit Theorem the variance of their average is $O(N^{-1})$. Consequently, the dominant contributions of both the bias and variance come from estimating $\mathbb{E}[r(x)]$. We show that μ_{PAQ} effectively implements a stochastic trapezoidal rule approximating r , where the randomness

comes from the labeled features. Based on the analysis of [58], we control the interpolation error using the derivative bounds of [Assumption 3](#) and carefully handle the error in the boundary regions, where $r(0)$ and $r(1)$ are unknown.

Remark 4 (Trapezoidal-Rule Interpretation; See [Lemma 7](#) in [Section E](#)). *It holds that*

$$\mu_{PAQ} = \frac{1}{N} \sum_{i=1}^N f(\tilde{x}_i) + x_1 \cdot r(x_1) + \sum_{i=1}^{n-1} (x_{i+1} - x_i) \cdot \frac{r(x_i) + r(x_{i+1})}{2} + (1 - x_n) \cdot r(x_n),$$

where $x_1 \leq \dots < x_n$ are the ordered labeled features.

6.1 Degree- p Polynomial Interpolation

So far, we approximated $\mathbb{E}[r(x)]$ by linear interpolation. To accelerate convergence, we replace the trapezoidal rule with degree- p polynomial interpolation, at the cost of the stronger smoothness assumptions below.

Assumption 4 (Smoothness for Degree- p Interpolation). *Let residual $r : \mathbb{R} \rightarrow \mathbb{R}$ be a deterministic residual function that is in C^{p+1} and such that $\sup_{x \in \mathbb{R}} |r^{(p+1)}(x)| \leq L$ for some finite constant L .*

To bound our approximation error using higher-order methods, we rely on the well-known Lagrange form of the remainder.

Fact 1. *Let x_1, \dots, x_p be n distinct points such that $a = x_0 < x_1 < \dots < x_p < x_{p+1} = b$. Suppose that the function r satisfies [Assumption 4](#) and let q_p be the unique degree p polynomial with*

$$q_p(x_i) = r(x_i), \quad i = 0, \dots, p.$$

Then, for each $x \in [a, b]$, there exists a ξ such that

$$r(x) - q_p(x) = \frac{r^{(p+1)}(\xi)}{(p+1)!} \prod_{i=0}^p (x - x_i).$$

Moreover, let $h = \max_{0 \leq i \leq p+1} (x_i - x_{i-1})$, then

$$\sup_{x \in [0, 1]} |r(x) - q_p(x)| \leq \frac{L_{p+1}}{(p+1)!} h^{p+1} = O(h^{p+1}).$$

Let $X_1 < X_2 < \dots < X_n$ be the order statistics of labeled features in \mathcal{L} . We will partition the interval $[0, 1]$ into $k+2$ intervals:

$$I_0 = [0, X_{p+1}], \quad I_j = [X_{(p+1)+d \cdot (i-1)}, x_{d+1, p \cdot i}] \quad 1 \leq i \leq k, \quad I_{k+1} = [X_{n-p}, 1],$$

where $k = (n - 2p - 1)/p$. Thus, each interval covers $p+1$ constructive order statistics. In each interval I_j , we fit a local degree- p polynomial $q_{j,p}$. The global interpolation q_p is then obtained by summing the regional approximations. Thus, the degree- p interpolation estimator becomes

$$\mu_{PAQ}^p = \frac{1}{N} \sum_{i=1}^N f(\tilde{X}_i) + \sum_{j=0}^{k+1} \int_{I_j} q_{j,p}(u) du.$$

Theorem 5 (PAQ Estimator, Degree- p Interpolation). *Under Assumption 4 with $p = O(1)$ and $P_X = \mathcal{U}_{[0,1]}$, it holds that*

$$|\mathbb{E}[\mu_{PAQ}^p] - \mathbb{E}[Y]| = O\left(\frac{1}{n^{p+1}}\right) \quad \text{and} \quad \text{Var}(\mu_{PAQ}^p) = O\left(\frac{1}{N} + \frac{1}{n^{2p+2}}\right).$$

Proof. We focus on bounding the bias and variance of $\sum_{j=0}^{k+1} \int_{I_j} q_{j,p}(u) du$. Recall that $\mathbb{E}[r(X)] = \int_0^1 r(u) du$ and $\mathbb{E}[q_p] = \mathbb{E}[\sum_i \int_{I_i} q_{i,p}(u) du]$. To bound the bias, we substitute these definitions in and calculate

$$\begin{aligned} |\mathbb{E}[q_p] - \mathbb{E}[r]| &= \left| \sum_{i=0}^{k+1} \mathbb{E} \left[\int_{I_i} q_{i,p}(u) - r(u) du \right] \right| \\ &\leq \sum_{i=0}^{k+1} \mathbb{E}[|I_i| \cdot \sup_{u \in I_i} |q_{i,p} - r|] \\ &\leq \frac{L}{p+1} \sum_{i=0}^{k+1} \mathbb{E}[|I_i|^{p+2}] \\ &= O\left(\frac{1}{n^{p+1}}\right), \end{aligned}$$

where the last inequality follows from Definition 1 and the last equality from $\mathbb{E}[|I_i|] = p/n = O(1/n)$. We may similarly bound variance by

$$\begin{aligned} \text{Var}(q_p) &= \text{Var}(q_p - E[r(x)]) \\ &= \text{Var} \left(\sum_i \int_{I_i} q_{i,p}(u) - r(u) du \right) \\ &\leq \text{Var} \left(\sum_i |I_i|^{p+2} \right) \\ &= \sum_i \text{Var}(|I_i|^{p+2}) + 2 \sum_{i < j} \text{Cov}(|I_i|^{p+2}, |I_j|^{p+2}) \\ &= O(n \cdot n^{-(2p+4)} + n^2 \cdot n^{-(2p+4)}) \\ &= O(n^{-(2p+2)}) \end{aligned}$$

The proof concludes by observing that $\text{Var}(\frac{1}{N} \sum_{i=1}^N f(\tilde{X}_i)) = O(1/N)$. \square

6.2 Beyond the Uniform Distribution and Applications to Higher Dimensions

We may apply the result of Theorem 5 to general distributions by applying the probability integral transformation. For an marginal distribution P_X in \mathbb{R} with a continuous CDF F , let

$$\tilde{r}(u) = r(F^{-1}(u)), \quad u \in [0, 1].$$

Then,

$$\mathbb{E}_{X \sim P_X}[r(X)] = \mathbb{E}_{U \sim \mathcal{U}_{[0,1]}}[\tilde{r}(u)]$$

by observing that $F(X_1), \dots, F(X_n)$ is distributed $U[0, 1]$. We can now apply the same numerical integration technique described in [Theorem 5](#) to $\tilde{r}(u)$, assuming that $\tilde{r}(u)$ satisfies [Assumption 4](#).

Since F is unknown in practice, one uses the empirical CDF

$$F_n(x) = n^{-1} \sum_{i=1}^n \mathbf{1}_{\tilde{X}_i \leq x}, \quad U_i = F_n(X_i).$$

We can bound the difference in the empirical and true CDF using the Dvoretzky–Kiefer–Wolfowitz (DKW) inequality.

Definition 1 (Dvoretzky–Kiefer–Wolfowitz (DKW) inequality [\[25, 38\]](#)). *Given n samples $(X_i)_{i=1}^n$ from a distribution D , the empirical distribution D_n with cdf $F_n(x) = n^{-1} \sum_{i=1}^n \mathbf{1}_{X_i \leq x}$ satisfies the following inequality:*

$$\Pr(d_{KS}(D_n, D) > \epsilon) \leq 2e^{-2n\epsilon^2}.$$

In particular, [Definition 1](#) implies that

$$|\sup_x |F_n(x) - F(x)|| = O(N^{-1/2}).$$

So, substituting F_n for F incurs at most $O(N^{-1/2})$ additional bias and $O(N^{-1})$ additional variance. Thus, we can safely use the empirical CDF without changing the final asymptotic rate.

We conclude this section with a brief remark about how our estimator μ_{PAQ}^p can be easily extended to when the feature space is d -dimensional. Concretely, suppose that $r : [0, 1]^d \rightarrow \mathbb{R}$ is a C^{p+1} function and we have access to a one-dimensional quadrature rule of order p computed on n nodes, denoted by

$$Q_1[f] = \sum_{i=1}^n w_i f(x_i),$$

which exactly integrates all polynomials of degree up to p . We may consider a d -dimensional quadrature rule by considering the

$$Q_d[f] = \sum_{i_1, \dots, i_d=1}^n w_{i_1} \cdot \dots \cdot w_{i_d} f(x_1, \dots, x_d),$$

which is exact for every multivariate monomial of degree at most p (see [\[15\]](#) for a standard reference). Since Q_d requires n^d points, this implies that the mesh size of the interpolation is $O(n^{1/d})$. We may substitute this bound into our previous analyses to yield the following result.

Theorem 6 (PAQ Estimator in d dimensions). *Suppose the residual $r : [0, 1]^d \rightarrow \mathbb{R}$ is in C^{p+1} and all $p+1$ order partial derivatives are bounded, then μ_{PAQ}^p with the quadrature rule $Q_d[f]$ satisfies*

$$|\mathbb{E}[\mu_{PAQ}^p] - \mathbb{E}[Y]| = O\left(\frac{1}{n^{(p+1)/d}}\right) \quad \text{and} \quad \text{Var}(\mu_{PAQ}^p) = O\left(\frac{1}{N} + \frac{1}{n^{(2p+2)/d}}\right).$$

6.3 Synthetic Experiments for the PAQ Estimator

In this section, we empirically test the PAQ estimator against PPI++ and PART, following the same testing methodology as [Section 5](#). While the PAQ estimator assumes that the residuals are deterministic and Lipschitz, there are many natural settings where the conditions of [Assumption 3](#) hold exactly or in good approximation. For example, Anfinsen’s thermodynamic hypothesis [3] suggests that for many small globular proteins under appropriate conditions the amino-acid sequence determines uniquely determines its physical structure. Similarly, in physics, there are many equations in which the final state of the system is determined by its initial conditions, such as in the 2-D incompressible Navier-Stokes equation [19].

In the experiments below, we first demonstrate the performance of the PAQ estimator on a synthetic dataset that exactly meets the assumptions of [Theorem 4](#) ([Figure 8](#)). We then show that the NN estimator is resilient to small amounts of noise ([Figure 9](#)). To construct our synthetic dataset, we let

$$X \sim \mathcal{U}[0, \pi], \quad y(x) = x^2 + \sin(x), \quad f(x) = x^2, \quad r(x) = \sin(x).$$

The residual function is deterministic and Lipschitz continuous with a constant of 1. The figures below show the average confidence interval width and the coverage probability as a function of the labeled sample size with a desired coverage probability of 0.9.

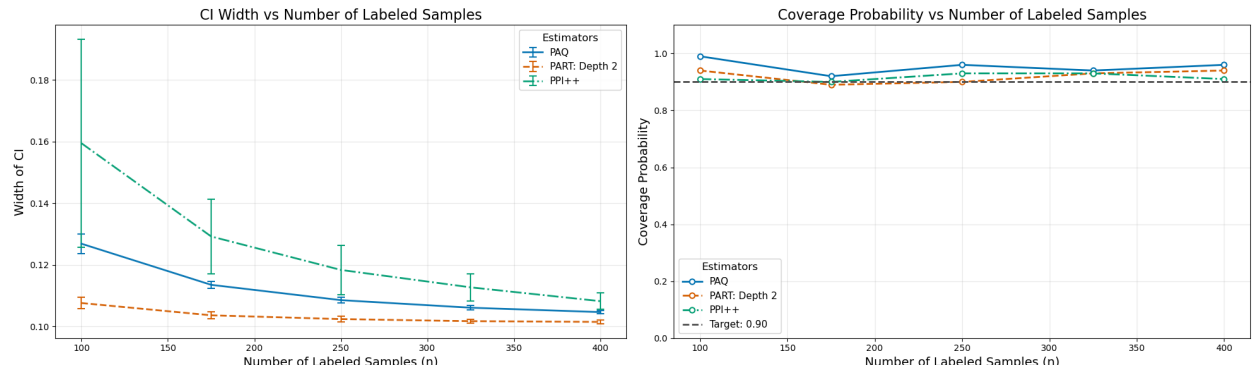


Figure 8: Estimating the mean on a synthetic dataset (see [Section 5](#) for testing methodology).

We now alter the previous example by introducing varying levels of noise to the labels. For $\sigma \in [0, 0.1, 0.2, 0.5, 1]$, we add $N(0, \sigma^2)$ noise to the labels in the previous examples. As expected, the coverage probability drops as the noise becomes more dominant in the label function.

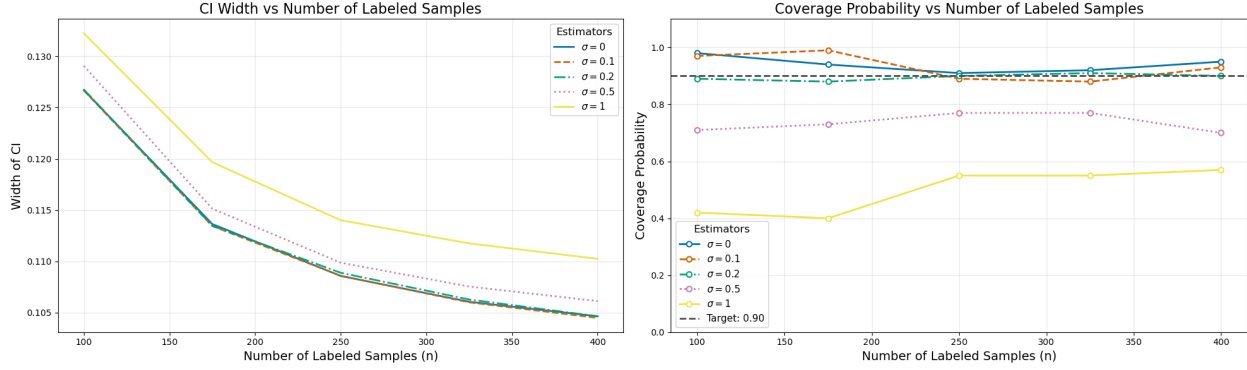


Figure 9: Testing the PAQ estimator’s efficacy with various noise levels in the response variable.

References

- [1] Algorithms with predictions. <https://algorithms-with-predictions.github.io/>, 2025. Accessed: 2025-09-15.
- [2] P. Agrawal, E. Balkanski, V. Gkatzelis, T. Ou, and X. Tan. Learning-augmented mechanism design: Leveraging predictions for facility location. In *Proceedings of the 23rd ACM Conference on Economics and Computation*, EC ’22, page 497–528, New York, NY, USA, 2022. Association for Computing Machinery. ISBN 9781450391504. doi: 10.1145/3490486.3538306. URL <https://doi.org/10.1145/3490486.3538306>.
- [3] C. B. Anfinsen. Principles that govern the folding of protein chains. *Science*, 181(4096): 223–230, July 1973.
- [4] A. N. Angelopoulos, S. Bates, C. Fannjiang, M. I. Jordan, and T. Zrnic. Prediction-powered inference. *Science*, 382(6671):669–674, 2023. doi: 10.1126/science.adi6000. URL <https://www.science.org/doi/abs/10.1126/science.adi6000>.
- [5] A. N. Angelopoulos, J. C. Duchi, and T. Zrnic. PPI++: Efficient Prediction-Powered Inference. *arXiv e-prints*, art. arXiv:2311.01453, Nov. 2023. doi: 10.48550/arXiv.2311.01453.
- [6] E. Balkanski, V. Gkatzelis, and G. Shahkarami. Randomized strategic facility location with predictions. In *Proceedings of the 38th International Conference on Neural Information Processing Systems*, NIPS ’24, Red Hook, NY, USA, 2025. Curran Associates Inc. ISBN 9798331314385.
- [7] E. Bampis, K. Dogeas, A. Kononov, G. Lucarelli, and F. Pascual. Scheduling with untrusted predictions. In L. D. Raedt, editor, *Proceedings of the Thirty-First International Joint Conference on Artificial Intelligence*, IJCAI-22, pages 4581–4587. International Joint Conferences on Artificial Intelligence Organization, 7 2022. doi: 10.24963/ijcai.2022/636. URL <https://doi.org/10.24963/ijcai.2022/636>. Main Track.

[8] B. Berger, M. Feldman, V. Gkatzelis, and X. Tan. Learning-augmented metric distortion via (p,q) -veto core. In *Proceedings of the 25th ACM Conference on Economics and Computation*, EC '24, page 984, New York, NY, USA, 2024. Association for Computing Machinery. ISBN 9798400707049. doi: 10.1145/3670865.3673456. URL <https://doi.org/10.1145/3670865.3673456>.

[9] F. D. Blau and L. M. Kahn. The gender wage gap: Extent, trends, and explanations. *Journal of Economic Literature*, 55(3):789–865, September 2017. doi: 10.1257/jel.20160995. URL <https://www.aeaweb.org/articles?id=10.1257/jel.20160995>.

[10] I. Bludau, S. Willems, W.-F. Zeng, M. T. Strauss, F. M. Hansen, M. C. Tanzer, O. Karayel, B. A. Schulman, and M. Mann. The structural context of posttranslational modifications at a proteome-wide scale. *PLoS Biol.*, 20(5):e3001636, May 2022.

[11] L. Breiman. Bagging predictors. *Mach. Learn.*, 24(2):123–140, Aug. 1996.

[12] L. Breiman. Random forests. *Mach. Learn.*, 45(1):5–32, Oct. 2001.

[13] L. Breiman, J. H. Friedman, R. A. Olshen, and C. J. Stone. *Classification And Regression Trees*. Routledge, Oct. 2017.

[14] E. L. Bullock, C. E. Woodcock, C. Souza Jr., and P. Olofsson. Satellite-based estimates reveal widespread forest degradation in the amazon. *Global Change Biology*, 26(5):2956–2969, 2020. doi: <https://doi.org/10.1111/gcb.15029>. URL <https://onlinelibrary.wiley.com/doi/abs/10.1111/gcb.15029>.

[15] R. Burden and J. Faires. *Numerical Analysis*. Brooks/Cole, Cengage Learning, 2011. ISBN 9780538735643. URL <https://books.google.com/books?id=KlfrjCDayHwC>.

[16] G. Carleo and M. Troyer. Solving the quantum many-body problem with artificial neural networks. *Science*, 355(6325):602–606, Feb. 2017.

[17] V. Chernozhukov, D. Chetverikov, M. Demirer, E. Duflo, C. Hansen, W. Newey, and J. Robins. Double/debiased machine learning for treatment and structural parameters. *Econom. J.*, 21(1):C1–C68, Feb. 2018.

[18] E. Cheung, E. Athanassoula, K. L. Masters, R. C. Nichol, A. Bosma, E. F. Bell, S. M. Faber, D. C. Koo, C. Lintott, T. Melvin, K. Schawinski, R. A. Skibba, and K. W. Willett. Galaxy zoo: Observing secular evolution through bars. *Astrophys. J.*, 779(2):162, Dec. 2013.

[19] P. Constantin and C. Foiaş. *Navier-stokes equations*. University of Chicago press, 1988.

[20] P. Cortez, A. Cerdeira, F. Almeida, T. Matos, and J. Reis. Wine Quality. UCI Machine Learning Repository, 2009. DOI: <https://doi.org/10.24432/C56S3T>.

[21] J. Dauparas, I. Anishchenko, N. Bennett, H. Bai, R. J. Ragotte, L. F. Milles, B. I. M. Wicky, A. Courbet, R. J. de Haas, N. Bethel, P. J. Y. Leung, T. F. Huddy, S. Pellock, D. Tischer, F. Chan, B. Koepnick, H. Nguyen, A. Kang, B. Sankaran, A. K. Bera,

N. P. King, and D. Baker. Robust deep learning-based protein sequence design using proteinmpnn. *Science*, 378(6615):49–56, 2022. doi: 10.1126/science.add2187. URL <https://www.science.org/doi/abs/10.1126/science.add2187>.

[22] S. Dieleman, K. W. Willett, and J. Dambre. Rotation-invariant convolutional neural networks for galaxy morphology prediction. *Monthly Notices of the Royal Astronomical Society*, 450(2):1441–1459, 04 2015. ISSN 0035-8711. doi: 10.1093/mnras/stv632. URL <https://doi.org/10.1093/mnras/stv632>.

[23] F. Ding, M. Hardt, J. Miller, and L. Schmidt. Retiring adult: new datasets for fair machine learning. In *Proceedings of the 35th International Conference on Neural Information Processing Systems*, NIPS ’21, Red Hook, NY, USA, 2021. Curran Associates Inc. ISBN 9781713845393.

[24] M. Dinitz, S. Im, T. Lavastida, B. Moseley, and S. Vassilvitskii. Algorithms with prediction portfolios. In *Proceedings of the 36th International Conference on Neural Information Processing Systems*, NIPS ’22, Red Hook, NY, USA, 2022. Curran Associates Inc. ISBN 9781713871088.

[25] A. Dvoretzky, J. Kiefer, and J. Wolfowitz. Asymptotic Minimax Character of the Sample Distribution Function and of the Classical Multinomial Estimator. *The Annals of Mathematical Statistics*, 27(3):642 – 669, 1956. doi: 10.1214/aoms/1177728174. URL <https://doi.org/10.1214/aoms/1177728174>.

[26] A. Geron. *Hands-On Machine Learning with Scikit-Learn, Keras, and TensorFlow: Concepts, Tools, and Techniques to Build Intelligent Systems*. O’Reilly Media, Inc., 2nd edition, 2019. ISBN 1492032646.

[27] E. Gibney and D. Castelvecchi. Physics nobel scooped by machine-learning pioneers. *Nature*, 634(8034):523–524, Oct. 2024.

[28] V. Gkatzelis, D. Schoepflin, and X. Tan. *Clock Auctions Augmented with Unreliable Advice*, pages 2629–2655. doi: 10.1137/1.9781611978322.86. URL <https://pubs.siam.org/doi/abs/10.1137/1.9781611978322.86>.

[29] S. Haber. A modified monte-carlo quadrature. ii. *Mathematics of Computation*, 21(99):388–397, 1967. ISSN 00255718, 10886842. URL <http://www.jstor.org/stable/2003241>.

[30] N. Jean, M. Burke, M. Xie, W. M. Alampay Davis, D. B. Lobell, and S. Ermon. Combining satellite imagery and machine learning to predict poverty. *Science*, 353(6301):790–794, Aug. 2016.

[31] J. Jumper, R. Evans, A. Pritzel, T. Green, M. Figurnov, O. Ronneberger, K. Tunyasuvunakool, R. Bates, A. Žídek, A. Potapenko, A. Bridgland, C. Meyer, S. A. A. Kohl, A. J. Ballard, A. Cowie, B. Romera-Paredes, S. Nikolov, R. Jain, J. Adler, T. Back, S. Petersen, D. Reiman, E. Clancy, M. Zielinski, M. Steinegger, M. Pacholska, T. Berghammer, S. Bodenstein, D. Silver, O. Vinyals, A. W. Senior, K. Kavukcuoglu, P. Kohli, and

D. Hassabis. Highly accurate protein structure prediction with AlphaFold. *Nature*, 596(7873):583–589, Aug. 2021.

[32] J. Kleinberg, H. Lakkaraju, J. Leskovec, J. Ludwig, and S. Mullainathan. Human decisions and machine predictions. *Q. J. Econ.*, 133(1):237–293, Feb. 2018.

[33] R. Lam, A. Sanchez-Gonzalez, M. Willson, P. Wirnsberger, M. Fortunato, F. Alet, S. Ravuri, T. Ewalds, Z. Eaton-Rosen, W. Hu, A. Merose, S. Hoyer, G. Holland, O. Vinyals, J. Stott, A. Pritzel, S. Mohamed, and P. Battaglia. Learning skillful medium-range global weather forecasting. *Science*, 382(6677):1416–1421, 2023. doi: 10.1126/science.adi2336. URL <https://www.science.org/doi/abs/10.1126/science.adi2336>.

[34] D. M. Lapola, P. Pinho, J. Barlow, L. E. O. C. Aragão, E. Berenguer, R. Carmenta, H. M. Liddy, H. Seixas, C. V. J. Silva, C. H. L. Silva-Junior, A. A. C. Alencar, L. O. Anderson, D. Armenteras, V. Brovkin, K. Calders, J. Chambers, L. Chini, M. H. Costa, B. L. Faria, P. M. Fearnside, J. Ferreira, L. Gatti, V. H. Gutierrez-Velez, Z. Han, K. Hibbard, C. Koven, P. Lawrence, J. Pongratz, B. T. T. Portela, M. Rounsevell, A. C. Ruane, R. Schaldach, S. S. da Silva, C. von Radow, and W. S. Walker. The drivers and impacts of amazon forest degradation. *Science*, 379(6630):eabp8622, 2023. doi: 10.1126/science.abp8622. URL <https://www.science.org/doi/abs/10.1126/science.abp8622>.

[35] Z. Lin, H. Akin, R. Rao, B. Hie, Z. Zhu, W. Lu, N. Smetanin, R. Verkuil, O. Kabeli, Y. Shmueli, A. dos Santos Costa, M. Fazel-Zarandi, T. Sercu, S. Candido, and A. Rives. Evolutionary-scale prediction of atomic-level protein structure with a language model. *Science*, 379(6637):1123–1130, 2023. doi: 10.1126/science.ade2574. URL <https://www.science.org/doi/abs/10.1126/science.ade2574>.

[36] W.-Y. Loh. Regression trees with unbiased variable selection and interaction detection. *Statistica Sinica*, 12(2):361–386, 2002. ISSN 10170405, 19968507. URL <http://www.jstor.org/stable/24306967>.

[37] T. Lykouris and S. Vassilvitskii. Competitive caching with machine learned advice. *J. ACM*, 68(4), July 2021. ISSN 0004-5411. doi: 10.1145/3447579. URL <https://doi.org/10.1145/3447579>.

[38] P. Massart. The Tight Constant in the Dvoretzky-Kiefer-Wolfowitz Inequality. *The Annals of Probability*, 18(3):1269 – 1283, 1990. doi: 10.1214/aop/1176990746. URL <https://doi.org/10.1214/aop/1176990746>.

[39] A. Merchant, S. Batzner, S. S. Schoenholz, M. Aykol, G. Cheon, and E. D. Cubuk. Scaling deep learning for materials discovery. *Nature*, 624(7990):80–85, Dec. 2023.

[40] M. Mohri, A. Rostamizadeh, and A. Talwalkar. *Foundations of machine learning*. MIT press, 2018.

[41] J. N. Morgan and J. A. Sonquist. Problems in the analysis of survey data, and a proposal. *Journal of the American Statistical Association*, 58(302):415–434, 1963. ISSN 01621459, 1537274X. URL <http://www.jstor.org/stable/2283276>.

[42] G. Ngo, R. Beard, and R. Chandra. Evolutionary bagging for ensemble learning. *Neurocomputing*, 510:1–14, 2022. ISSN 0925-2312. doi: <https://doi.org/10.1016/j.neucom.2022.08.055>. URL <https://www.sciencedirect.com/science/article/pii/S0925231222010414>.

[43] E. Nguyen, M. Poli, M. G. Durrant, B. Kang, D. Katrekar, D. B. Li, L. J. Bartie, A. W. Thomas, S. H. King, G. Brixi, J. Sullivan, M. Y. Ng, A. Lewis, A. Lou, S. Ermon, S. A. Baccus, T. Hernandez-Boussard, C. Ré, P. D. Hsu, and B. L. Hie. Sequence modeling and design from molecular to genome scale with evo. *Science*, 386(6723):eado9336, 2024. doi: [10.1126/science.ado9336](https://doi.org/10.1126/science.ado9336). URL <https://www.science.org/doi/abs/10.1126/science.ado9336>.

[44] A. Omidi, M. H. Møller, N. Malhis, J. M. Bui, and J. Gsponer. AlphaFold-multimer accurately captures interactions and dynamics of intrinsically disordered protein regions. *Proceedings of the National Academy of Sciences*, 121(44):e2406407121, 2024. doi: [10.1073/pnas.2406407121](https://doi.org/10.1073/pnas.2406407121). URL <https://www.pnas.org/doi/abs/10.1073/pnas.2406407121>.

[45] R. K. Pace and R. Barry. Sparse spatial autoregressions. *Statistics & Probability Letters*, 33(3):291–297, 1997. ISSN 0167-7152. doi: [https://doi.org/10.1016/S0167-7152\(96\)00140-X](https://doi.org/10.1016/S0167-7152(96)00140-X). URL <https://www.sciencedirect.com/science/article/pii/S016771529600140X>.

[46] A. Philippe. Processing simulation output by riemann sums. *J. Stat. Comput. Simul.*, 59(4):295–314, Dec. 1997.

[47] C. Piech, J. Bassen, J. Huang, S. Ganguli, M. Sahami, L. J. Guibas, and J. Sohl-Dickstein. Deep knowledge tracing. In C. Cortes, N. Lawrence, D. Lee, M. Sugiyama, and R. Garnett, editors, *Advances in Neural Information Processing Systems*, volume 28. Curran Associates, Inc., 2015. URL https://proceedings.neurips.cc/paper_files/paper/2015/file/bac9162b47c56fc8a4d2a519803d51b3-Paper.pdf.

[48] J. O. Sexton, X.-P. Song, M. Feng, P. Noojipady, A. Anand, C. Huang, D.-H. Kim, K. M. Collins, S. Channan, C. DiMiceli, and J. R. Townshend. Global, 30-m resolution continuous fields of tree cover: Landsat-based rescaling of modis vegetation continuous fields with lidar-based estimates of error. *International Journal of Digital Earth*, 6(5):427–448, 2013. doi: [10.1080/17538947.2013.786146](https://doi.org/10.1080/17538947.2013.786146). URL <https://doi.org/10.1080/17538947.2013.786146>.

[49] C. J. Shallue and A. Vanderburg. Identifying Exoplanets with Deep Learning: A Five-planet Resonant Chain around Kepler-80 and an Eighth Planet around Kepler-90. *Astronomical Journal*, 155(2):94, Feb. 2018. doi: [10.3847/1538-3881/aa9e09](https://doi.org/10.3847/1538-3881/aa9e09).

[50] T. Shen, Z. Hu, S. Sun, D. Liu, F. Wong, J. Wang, J. Chen, Y. Wang, L. Hong, J. Xiao, L. Zheng, T. Krishnamoorthi, I. King, S. Wang, P. Yin, J. J. Collins, and Y. Li. Accurate RNA 3D structure prediction using a language model-based deep learning approach. *Nat. Methods*, 21(12):2287–2298, Dec. 2024.

[51] J. M. Stokes, K. Yang, K. Swanson, W. Jin, A. Cubillos-Ruiz, N. M. Donghia, C. R. MacNair, S. French, L. A. Carfrae, Z. Bloom-Ackermann, V. M. Tran, A. Chiappino-Pepe, A. H. Badran, I. W. Andrews, E. J. Chory, G. M. Church, E. D. Brown, T. S. Jaakkola, R. Barzilay, and J. J. Collins. A deep learning approach to antibiotic discovery. *Cell*, 180(4):688–702.e13, Feb. 2020.

[52] K. Tunyasuvunakool, J. Adler, Z. Wu, T. Green, M. Zielinski, A. Žídek, A. Bridgland, A. Cowie, C. Meyer, A. Laydon, S. Velankar, G. J. Kleywegt, A. Bateman, R. Evans, A. Pritzel, M. Figurnov, O. Ronneberger, R. Bates, S. A. A. Kohl, A. Potapenko, A. J. Ballard, B. Romera-Paredes, S. Nikolov, R. Jain, E. Clancy, D. Reiman, S. Petersen, A. W. Senior, K. Kavukcuoglu, E. Birney, P. Kohli, J. Jumper, and D. Hassabis. Highly accurate protein structure prediction for the human proteome. *Nature*, 596(7873):590–596, Aug. 2021.

[53] UniProt Consortium. UniProt: a hub for protein information. *Nucleic Acids Res.*, 43 (Database issue):D204–12, Jan. 2015.

[54] A. W. v. d. Vaart. *Asymptotic Statistics*. Cambridge Series in Statistical and Probabilistic Mathematics. Cambridge University Press, 1998.

[55] H. Wang, T. Fu, Y. Du, W. Gao, K. Huang, Z. Liu, P. Chandak, S. Liu, P. Van Katwyk, A. Deac, A. Anandkumar, K. Bergen, C. P. Gomes, S. Ho, P. Kohli, J. Lasenby, J. Leskovec, T.-Y. Liu, A. Manrai, D. Marks, B. Ramsundar, L. Song, J. Sun, J. Tang, P. Veličković, M. Welling, L. Zhang, C. W. Coley, Y. Bengio, and M. Zitnik. Scientific discovery in the age of artificial intelligence. *Nature*, 620(7972):47–60, Aug. 2023.

[56] K. W. Willett, C. J. Lintott, S. P. Bamford, K. L. Masters, B. D. Simmons, K. R. V. Casteels, E. M. Edmondson, L. F. Fortson, S. Kaviraj, W. C. Keel, T. Melvin, R. C. Nichol, M. J. Raddick, K. Schawinski, R. J. Simpson, R. A. Skibba, A. M. Smith, and D. Thomas. Galaxy zoo 2: detailed morphological classifications for 304,122 galaxies from the sloan digital sky survey. *Monthly Notices of the Royal Astronomical Society*, 435(4):2835–2860, 09 2013. ISSN 0035-8711. doi: 10.1093/mnras/stt1458. URL <https://doi.org/10.1093/mnras/stt1458>.

[57] C. J. Wilson, W.-Y. Choy, and M. Karttunen. AlphaFold2: A role for disordered protein/region prediction? *Int. J. Mol. Sci.*, 23(9):4591, Apr. 2022.

[58] S. Yakowitz, J. E. Krimmel, and F. Szidarovszky. Weighted monte carlo integration. *SIAM Journal on Numerical Analysis*, 15(6):1289–1300, 1978. doi: 10.1137/0715088. URL <https://doi.org/10.1137/0715088>.

[59] D. G. York, et al. The Sloan Digital Sky Survey: Technical Summary. *Astronomical Journal*, 120(3):1579–1587, Sept. 2000. doi: 10.1086/301513.

- [60] B. Zhu, M. Ding, P. Jacobson, M. Wu, W. Zhan, M. Jordan, and J. Jiao. Doubly-robust self-training. In A. Oh, T. Naumann, A. Globerson, K. Saenko, M. Hardt, and S. Levine, editors, *Advances in Neural Information Processing Systems*, volume 36, pages 41413–41431. Curran Associates, Inc., 2023. URL https://proceedings.neurips.cc/paper_files/paper/2023/file/819f426947c27eb5067bb6fdbdde93dd-Paper-Conference.pdf.
- [61] T. Zrnic. A note on the prediction-powered bootstrap, 2025. URL <https://arxiv.org/abs/2405.18379>.
- [62] T. Zrnic and E. J. Candès. Cross-prediction-powered inference. *Proceedings of the National Academy of Sciences*, 121(15):e2322083121, 2024. doi: 10.1073/pnas.2322083121. URL <https://www.pnas.org/doi/abs/10.1073/pnas.2322083121>.

A Algorithms

In this section, we present the PART algorithm for mean estimation and linear regression. At their core, both algorithms build a regression tree by repeatedly splitting the labeled data in a greedy fashion. Once the tree is formed, local residuals are computed within each leaf using the labeled data and the leaf mixture probabilities are computed using the unlabeled data assigned to each leaf. We also provide the PAQ algorithm for mean estimation, which computes the global residual term by assigning each unlabeled point the residual of its nearest labeled neighbor.

Algorithm 1 PART Mean Estimator

Require:

- 1:
 - Labeled data $\mathcal{L} = \{(x_i, y_i)\}_{i=1}^n$,
 - Unlabeled data $\mathcal{U} = \{\tilde{x}_j\}_{j=1}^N$,
 - Predictor $f : \mathcal{X} \rightarrow \mathbb{R}$,
 - Maximum depth D , and minimum labeled sample size m .
- 2: Initialize the root region: $\mathcal{R} \leftarrow \mathcal{X}$.
- 3: **function** BUILDTREE(\mathcal{R} , depth)
- 4: **if** depth = D **or** $|\mathcal{L} \cap \mathcal{R}| < m$ **then**
- 5: **return** \mathcal{R}
- 6: **end if**
- 7: Determine the optimal split coordinate $k^* \in [1, d]$, and split point $s^* \in \mathcal{S}^{(k)}$ on \mathcal{R} that minimizes the VMS function $\text{VMS}(k^*, s^*, \mathcal{R})$. (see paragraphs **Candidate Splitting Points** and **Splitting Function** in [Section 4.1](#)).
- 8: Partition \mathcal{R} into $\mathcal{R}_{\text{left}} = \{x \in \mathcal{R} : x^{(k^*)} \leq s^*\}$ and $\mathcal{R}_{\text{right}} = \{x \in \mathcal{R} : x^{(k^*)} > s^*\}$.
- 9: **return** BUILDTREE($\mathcal{R}_{\text{left}}$, depth + 1) \cup BUILDTREE($\mathcal{R}_{\text{right}}$, depth + 1).
- 10: **end function**
- 11: Build the tree: $T \leftarrow \text{BUILDTREE}(\mathcal{X}, 0)$.
- 12: Let $\{\mathcal{R}_\ell\}_{\ell=1}^L$ be the leaf regions of T . For each leaf \mathcal{R}_ℓ , compute:
 - $p_\ell = |\{\tilde{x} \in \mathcal{U} \cap \mathcal{R}_\ell\}|/N$,
 - $\bar{r}_\ell = \frac{1}{|\mathcal{L} \cap \mathcal{R}_\ell|} \sum_{(x,y) \in \mathcal{L} \cap \mathcal{R}_\ell} r(x, y)$.
- 13: **return** the final estimator $\hat{\mu}_T = \frac{1}{N} \sum_{j=1}^N f(\tilde{x}_j) + \sum_{\ell=1}^L p_\ell \bar{r}_\ell$.

Algorithm 2 PART Tree Estimator for Linear Regression

Require:

- 1:
 - Labeled data $\mathcal{L} = \{(x_i, y_i)\}_{i=1}^n$,
 - Unlabeled data $\mathcal{U} = \{\tilde{x}_j\}_{j=1}^N$,
 - Predictor function $f : \mathcal{X} \rightarrow \mathbb{R}$,
 - Maximum depth D , minimum labeled sample size m , and coordinate k for coefficient estimation.
- 2: Initialize the root region: $\mathcal{R} \leftarrow \mathcal{X}$.
- 3: **function** BUILDTREE(\mathcal{R} , depth)
- 4: **if** depth = D **or** $|\mathcal{L} \cap \mathcal{R}| < m$ **then**
- 5: **return** \mathcal{R}
- 6: **end if**
- 7: Determine the optimal split coordinate $j^* \in [1, d]$, and split point $s^* \in \mathcal{S}^{(j^*)}$ on \mathcal{R} that minimizes $\text{VMS}_{\text{LR}}(j^*, s^*, \mathcal{R})$ (see paragraphs **Candidate Splitting Points** in [Section 4.1](#) and **Splitting Function for Linear Regression** in [Section 4.2](#)).
- 8: Partition \mathcal{R} into $\mathcal{R}_{\text{left}} = \{x \in \mathcal{R} : x^{(j^*)} \leq s^*\}$ and $\mathcal{R}_{\text{right}} = \{x \in \mathcal{R} : x^{(j^*)} > s^*\}$.
- 9: **return** BUILDTREE($\mathcal{R}_{\text{left}}$, depth + 1) \cup BUILDTREE($\mathcal{R}_{\text{right}}$, depth + 1).
- 10: **end function**
- 11: Build the tree: $T \leftarrow \text{BUILDTREE}(\mathcal{X}, 0)$.
- 12: Let $\{\mathcal{R}_\ell\}_{\ell=1}^L$ be the leaf regions of T . For each leaf \mathcal{R}_ℓ , compute:
 - $p_{\mathcal{R}_\ell} = |\{\tilde{x} \in \mathcal{U} \cap \mathcal{R}_\ell\}|/N$,
 - $\hat{R}_{\mathcal{R}_\ell}^{(k)} = \left(\frac{1}{N} \sum_{i=1}^N \tilde{x}_i \tilde{x}_i^T \right)^{-1} \frac{1}{|\mathcal{L} \cap \mathcal{R}_\ell|} \sum_{(x,y) \in \mathcal{L} \cap \mathcal{R}_\ell} x^{(k)} (y - f(x))$.
- 13: Compute predictor-augmented estimator $\tilde{\theta}^{(k)} = \left(\frac{1}{N} \sum_{i=1}^N \tilde{x}_i \tilde{x}_i^T \right)^{-1} \frac{1}{N} \sum_{i=1}^N \tilde{x}_i f(\tilde{x}_i)$.
- 14: **return** final estimator $\hat{\theta}_T^{(k)} = \tilde{\theta}^{(k)} + \sum_{\ell=1}^L p_{\mathcal{R}_\ell} \hat{R}_{\mathcal{R}_\ell}^{(k)}$.

Algorithm 3 PAQ Mean Estimator

Require:

- 1:
 - Labeled data $\mathcal{L} = \{(x_i, y_i)\}_{i=1}^n$,
 - Unlabeled data $\mathcal{U} = \{\tilde{x}_j\}_{j=1}^N$,
 - Predictor $f : \mathcal{X} \rightarrow \mathbb{R}$,
- 2: **function** NEARESTLABELEDNEIGHBOR(\tilde{x} , \mathcal{L})
- 3: **return** $\arg \min_{x \in \mathcal{L}} |\tilde{x} - x|$.
- 4: **end function**
- 5: **return** the final estimator $\hat{\mu}_{\text{PAQ}} = \frac{1}{N} \sum_{j=1}^N (f(\tilde{x}_j) + \text{NEARESTLABELEDNEIGHBOR}(\tilde{x}_j, \mathcal{L}))$.

B Proof of Lemma 1

In this section, we restate and prove [Lemma 1](#), which shows that [Estimator 1](#) goes asymptotically to a normal distribution with controlled variance.

Lemma 1 (Properties of [Estimator 1](#)). *Let $\hat{\mu}_C$ be the estimate from [Estimator 1](#), and assume $N \gg n$. Then $\hat{\mu}_C$ is an unbiased estimator for the mean $\mu = \mathbb{E}[Y]$. Moreover, when $\text{Var}(Y - f(X))$ is finite, and as $n \rightarrow \infty$,*

$$\sqrt{n} (\hat{\mu}_C - \mu) \xrightarrow{d} \mathcal{N}(0, \sigma_C^2), \text{ where } \sigma_C^2 := \sum_{x \in \{-1, 1\}} \Pr[X = x] \cdot \text{Var}(Y - f(X) \mid X = x).$$

Proof of [Lemma 1](#). Unbiasedness. Recall that for a binary feature $X \in \{-1, 1\}$, the coordinate-partition estimator is

$$\hat{\mu}_C = \underbrace{\frac{1}{N} \sum_{j=1}^N f(\tilde{x}_j)}_{\text{predictive term}} + \underbrace{\sum_{x \in \{-1, 1\}} \hat{p}_x \hat{r}_x}_{\text{group-specific residual correction}},$$

Because $N \gg n$ and $N \rightarrow \infty$, we treat

$$\frac{1}{N} \sum_{j=1}^N f(\tilde{x}_j) \xrightarrow{p} \mathbb{E}[f(X)], \quad \hat{p}_x \xrightarrow{p} \Pr[X = x].$$

Thus [Estimator 1](#) simplifies to

$$\mathbb{E}[f(X)] + \sum_{x \in \{-1, 1\}} \Pr[X = x] \hat{r}_x.$$

Notice that for each $x \in \{-1, 1\}$,

$$\mathbb{E}[\hat{r}_x] = \mathbb{E} \left[\frac{1}{n_x} \sum_{\{i: x_i=x\}} (y_i - f(x_i)) \right] = \mathbb{E}[Y - f(X) \mid X = x]$$

Hence by linearity of expectation we have that

$$\mathbb{E}[\hat{\mu}_C] = \mathbb{E}[f(X)] + \mathbb{E}[Y - f(X)] = \mathbb{E}[Y] = \mu.$$

Therefore, $\hat{\mu}_C$ is unbiased for μ .

Asymptotic Normality and Variance. As argued, [Estimator 1](#) in the limit becomes

$$\mathbb{E}[f(X)] + \sum_{x \in \{-1, 1\}} \Pr[X = x] \hat{r}_x.$$

Thus the main source of variability arises from the group-specific corrections \hat{r}_1 and \hat{r}_{-1} .

By assumption that $\text{Var}(Y - f(x))$ is finite, applying the CLT separately to each group we get:

$$\sqrt{n_x} (\hat{r}_x - \mathbb{E}[Y - f(X) \mid X = x]) \xrightarrow{d} \mathcal{N}(0, \text{Var}(Y - f(X) \mid X = x)).$$

To calculate the variance of [Estimator 1](#), we use the following claim that shows that the covariance between \hat{r}_{-1} and \hat{r}_1 is zero.

Claim 3. $\text{Cov}(\widehat{r}_{-1}, \widehat{r}_1) = 0$

Proof. We show that $\mathbb{E}[\widehat{r}_1 \cdot \widehat{r}_{-1}] = \mathbb{E}[\widehat{r}_1] \cdot \mathbb{E}[\widehat{r}_{-1}]$. From this, it follows immediately that $\text{Cov}(\widehat{r}_{-1}, \widehat{r}_1) = 0$. Consider the chain of equalities:

$$\begin{aligned}
& \mathbb{E}[\widehat{r}_1 \widehat{r}_{-1}] \\
&= \mathbb{E}[\mathbb{E}[\widehat{r}_1 \widehat{r}_{-1} \mid n_1, n_{-1}]] && \text{(law of total expectation)} \\
&= \mathbb{E}[\mathbb{E}[\widehat{r}_1 \mid n_1, n_{-1}] \mathbb{E}[\widehat{r}_{-1} \mid n_1, n_{-1}]] && \text{(conditional independence given } n_1, n_{-1} \text{)} \\
&= \mathbb{E}[\mathbb{E}[\widehat{r}_1 \mid n_1] \mathbb{E}[\widehat{r}_{-1} \mid n_{-1}]] && \text{(\widehat{r}_1 depends only on } n_1; \widehat{r}_{-1} \text{ only on } n_{-1} \text{)} \\
&= \mathbb{E}[\mathbb{E}[Y - f(X) \mid X = 1] \mathbb{E}[Y - f(X) \mid X = -1]] && \text{(\widehat{r}_1, \widehat{r}_{-1} \text{ are unbiased estimators)} \\
&= \mathbb{E}[Y - f(X) \mid X = 1] \mathbb{E}[Y - f(X) \mid X = -1] && \text{(constants with respect to the outer expectation)} \\
&= \mathbb{E}[\widehat{r}_1] \mathbb{E}[\widehat{r}_{-1}].
\end{aligned}$$

Hence $\mathbb{E}[\widehat{r}_1 \widehat{r}_{-1}] = \mathbb{E}[\widehat{r}_1] \mathbb{E}[\widehat{r}_{-1}]$, which implies

$$\text{Cov}(\widehat{r}_1, \widehat{r}_{-1}) = \mathbb{E}[\widehat{r}_1 \widehat{r}_{-1}] - \mathbb{E}[\widehat{r}_1] \mathbb{E}[\widehat{r}_{-1}] = 0.$$

□

Since the covariance between \widehat{r}_{-1} and \widehat{r}_1 is zero, the variance of [Estimator 1](#) is equal to

$$\begin{aligned}
& \sum_{x \in \{-1, 1\}} \Pr[X = x]^2 \cdot \frac{\text{Var}(Y - f(X) \mid X = x)}{n_x} \\
&= \sum_{x \in \{-1, 1\}} \left(\frac{\Pr[X = x]}{\frac{n_x}{n}} \right) \cdot \frac{\Pr[X = x] \cdot \text{Var}(Y - f(X) \mid X = x)}{n} \\
&\rightarrow \sum_{x \in \{-1, 1\}} \frac{\Pr[X = x] \cdot \text{Var}(Y - f(X) \mid X = x)}{n}
\end{aligned}$$

where in the last equality we applied Slutsky's theorem since $\frac{n_x}{n} \rightarrow \widehat{p}_x$ as $n \rightarrow \infty$.

□

C Proof of [Theorem 1](#)

In this section, we establish the asymptotic coverage of [Algorithm 1](#). To accomplish this, we define some additional notation and prove some helpful auxiliary claims.

Additional Notation: Let $\mu = \mathbb{E}[Y]$ be the true population mean. Define \mathcal{T}_L as the collection of all binary decision trees on \mathcal{X} formed by splitting along any coordinate $k \in \{1, \dots, d\}$ at threshold points in $\mathcal{S}^{(k)}$.

For a fixed tree $T \in \mathcal{T}_L$, let $\{\mathcal{R}_\ell\}_{\ell=1}^L$ denote its leaf regions. For each leaf $\ell \in \{1, \dots, L\}$, define:

- The *population mean* of the residuals using labelled data in \mathcal{R}_ℓ as μ_ℓ , and the corresponding empirical mean as $\hat{\mu}_\ell$.
- The *population variance* of the residuals as σ_ℓ^2 , with $\hat{\sigma}_\ell^2$ the corresponding *empirical variance* of the residuals using only labeled data in \mathcal{R}_ℓ .
- The *mass function* in subregion \mathcal{R}_ℓ as $p_\ell := \Pr[X \in \mathcal{R}_\ell]$.

Denote by $\hat{\mu}_T$ the PART estimator from Algorithm 1 associated with T . We write $\sigma_T^2 = \text{Var}(\hat{\mu}_T)$ for the *population variance* of $\hat{\mu}_T$, and $\hat{\sigma}_T^2$ for its *empirical variance*, following the definitions in the paragraph **Constructing Confidence Intervals** of Section 4.1.

Theorem 7. *The total number of distinct trees in \mathcal{T}_L is bounded by $|\mathcal{T}_L| \leq (d \cdot n)^L$.*

Proof. Let $T \in \mathcal{T}_L$ be a binary decision tree with exactly L leaves. It is well-known that a full binary tree with L leaves has $L - 1$ internal (non-leaf) nodes. Label these internal nodes as v_1, \dots, v_{L-1} .

Each internal node v_i requires two choices:

1. *Choice of feature:* There are d features from which to choose.
2. *Choice of threshold:* There are at most $n - 1$ thresholds.

Therefore, there are at most $d \cdot n$ possible splitting rules at each internal node. Since there are $L - 1$ internal nodes, the number of ways to specify *all* splitting rules for T is at most

$$(d \cdot n)^{L-1}.$$

Finally, since $(d \cdot n)^{L-1} \leq (d \cdot n)^L$ for $d, n, L \geq 1$, we obtain

$$|\mathcal{T}_L| \leq (d \cdot n)^L,$$

as claimed. □

Theorem 8 (Asymptotic Normality). *As $n \rightarrow \infty$, for any decision tree $T \in \mathcal{T}_L$, and $\delta \in (0, 1)$:*

$$\hat{\mu}_T \xrightarrow{d} N\left(\mathbb{E}[Y - f(x)], \frac{1}{n} \sum_{\ell=1}^L p_\ell \cdot \sigma_\ell^2\right), \text{ and } \Pr\left[\hat{\sigma}_T^2 \geq \sigma_T^2 \left(1 - 2\sqrt{\frac{\log(\frac{1}{\delta})}{n}}\right)\right] \geq 1 - \delta.$$

Proof. **Normality of $\hat{\mu}_T$:** We first compute the expected value and variance of $\hat{\mu}_T$:

$$\mathbb{E}[\hat{\mu}_T] = \sum_{\ell=1}^L p_\ell \mathbb{E}[\hat{\mu}_\ell] = \sum_{\ell=1}^L p_\ell \mu_\ell = \sum_{\ell=1}^L \Pr[X \in \mathcal{R}_\ell] \mathbb{E}[Y - f(X) \mid X \in \mathcal{R}_\ell] = \mathbb{E}[Y - f(X)],$$

where we use that $\hat{\mu}_\ell$ is an unbiased estimator of μ_ℓ . To compute the variance of $\hat{\mu}_T$, we use the following claim.

Claim 4. *For any pair of leafs $\ell \neq \ell'$, $\text{Cov}(\hat{\mu}_\ell, \hat{\mu}_{\ell'}) = 0$*

Proof Sketch. The proof follows similar to [Claim 3](#). □

Hence, the variance of $\hat{\mu}_T$ is

$$\text{Var}(\hat{\mu}_T) = \text{Var}\left(\sum_{\ell=1}^L p_\ell \hat{\mu}_\ell\right) = \sum_{\ell=1}^L p_\ell^2 \text{Var}(\hat{\mu}_\ell) = \sum_{\ell=1}^L p_\ell^2 \frac{\sigma_\ell^2}{n_\ell} = \frac{1}{n} \sum_{\ell=1}^L p_\ell^2 \frac{\sigma_\ell^2}{\frac{n_\ell}{n}} = \frac{1}{n} \sum_{\ell=1}^L p_\ell \sigma_\ell^2,$$

where we used that for $\ell \neq \ell'$, $\text{Cov}(\hat{\mu}_\ell, \hat{\mu}_{\ell'}) = 0$, and that the variance of n' i.i.d. random variables with variance σ' is $\frac{\sigma'^2}{n'^2}$. For the last equality we use that as $n \rightarrow \infty$, for each subregion \mathcal{R}_ℓ , if $p_\ell = 0$ then $n_\ell = 0$, otherwise $n_\ell \rightarrow +\infty$, hence $\lim_{n \rightarrow \infty} \frac{n_\ell}{n} = p_\ell$.

The first part of the argument follows from the CLT. By [Assumption 1](#), the average $\frac{1}{n} \sum_{\ell=1}^L p_\ell \sigma_\ell^2$ is finite, being a mean of finite values. Consequently, we have

$$\hat{\mu}_T \xrightarrow{d} N\left(\mathbb{E}[Y - f(x)], \frac{1}{n} \sum_{\ell=1}^L p_\ell \sigma_\ell^2\right).$$

Distribution of the Empirical Variance: For each leaf ℓ , since the n_ℓ observations are i.i.d., a standard result shows that the empirical variance $\hat{\sigma}_\ell^2$ satisfies

$$\frac{1}{n} \sum_{\ell=1}^L p_\ell \hat{\sigma}_\ell^2 \xrightarrow{d} \frac{1}{n} \sum_{\ell=1}^L p_\ell \sigma_\ell^2 \cdot \frac{\chi_{n_\ell-1}^2}{n_\ell-1} = \frac{1}{n} \sum_{\ell=1}^L p_\ell \sigma_\ell^2 + \frac{1}{n} \sum_{\ell=1}^L p_\ell \sigma_\ell^2 \cdot \frac{\chi_{n_\ell-1}^2 - (n_\ell-1)}{n_\ell-1}$$

Observe the following chain of reduction:

$$\begin{aligned}
\frac{1}{n} \sum_{\ell=1}^L p_\ell \hat{\sigma}_\ell^2 - \frac{1}{n} \sum_{\ell=1}^L p_\ell \sigma_\ell^2 &\xrightarrow{d} \sum_{\ell=1}^L \frac{p_\ell^2 \cdot \sigma_\ell^2}{n_\ell} \cdot \frac{\chi_{n_\ell-1}^2 - (n_\ell - 1)}{n_\ell - 1} \\
&= \sum_{\ell=1}^L \frac{\sqrt{2} \cdot p_\ell^2 \cdot \sigma_\ell^2}{n_\ell \cdot \sqrt{n_\ell - 1}} \cdot \frac{\chi_{n_\ell-1}^2 - (n_\ell - 1)}{\sqrt{2(n_\ell - 1)}} \\
&\xrightarrow{d} \sum_{\ell=1}^L \frac{\sqrt{2} \cdot p_\ell^2 \cdot \sigma_\ell^2}{n_\ell \cdot \sqrt{n_\ell - 1}} \cdot \mathcal{N}(0, 1) \\
&= \frac{\sqrt{2}}{n^{3/2}} \sum_{\ell=1}^L \frac{p_\ell^2 \cdot \sigma_\ell^2}{\frac{n_\ell}{n} \cdot \sqrt{\frac{n_\ell-1}{n}}} \cdot \mathcal{N}(0, 1) \\
&= \frac{\sqrt{2}}{n^{3/2}} \sum_{\ell=1}^L \sqrt{p_\ell} \cdot \sigma_\ell^2 \cdot \mathcal{N}(0, 1) \\
&= \mathcal{N} \left(0, \frac{2}{n^3} \sum_{\ell=1}^L p_\ell \cdot \sigma_\ell^4 \right),
\end{aligned}$$

where to derive the reductions we applied CLT on $\frac{\chi_{n_\ell-1}^2 - (n_\ell - 1)}{\sqrt{2(n_\ell - 1)}}$ $\xrightarrow{d} \mathcal{N}(0, 1)$, and applied Slutsky's theorem since $\frac{n_\ell-1}{n} \xrightarrow{d} p_\ell$.⁵ Hence, $\hat{\sigma}_T^2 - \frac{1}{n} \sum_{\ell=1}^L p_\ell \cdot \sigma_\ell^2 = \hat{\sigma}_T^2 - \sigma_T^2$ is distributed as $\mathcal{N} \left(0, \frac{2}{n^3} \cdot \sum_{\ell=1}^L p_\ell \cdot \sigma_\ell^4 \right)$. We use the following simple concentration bound for Gaussian distributions:

Claim 5 (Folklore). $\Pr_{X \sim N(0, \sigma'^2)}[X \leq -t] \leq \exp \left(-\frac{t^2}{2\sigma'^2} \right)$.

Hence for $t = \frac{2\sqrt{-\log(\delta)}}{n^{3/2}} \cdot \sum_{\ell=1}^L p_\ell \cdot \sigma_\ell^2 = 2 \cdot \sqrt{\frac{-\log(\delta)}{n}} \cdot \sigma_T^2$:

$$\begin{aligned}
\Pr \left[\hat{\sigma}_T^2 - \sigma_T^2 \leq -2\sqrt{\frac{-\log(\delta)}{n}} \sigma_T^2 \right] &\leq \exp \left(\log(\delta) \cdot \frac{\left(\sum_{\ell=1}^L p_\ell \sigma_\ell^2 \right)^2}{\sum_{\ell=1}^L p_\ell \sigma_\ell^4} \right) \\
&\leq \exp(\log(\delta)) = \delta \\
\Rightarrow \Pr \left[\hat{\sigma}_T^2 \leq \sigma_T^2 \left(1 - 2\sqrt{\frac{-\log(\delta)}{n}} \right) \right] &\leq \delta
\end{aligned}$$

Hence, $\Pr \left[\hat{\sigma}_T^2 \geq \sigma_T^2 \left(1 - 2\sqrt{\frac{-\log(\delta)}{n}} \right) \right] = 1 - \Pr \left[\hat{\sigma}_T^2 \leq \sigma_T^2 \left(1 - 2\sqrt{\frac{-\log(\delta)}{n}} \right) \right] \geq 1 - \delta$, concludes the proof. \square

⁵ Requirements of CLT are satisfied, since as argued before if $p_\ell = 0$ then $n_\ell = 0$, otherwise $n_\ell \rightarrow +\infty$, and since $\frac{\chi_{n_\ell-1}^2 - (n_\ell - 1)}{\sqrt{2(n_\ell - 1)}}$ has unit variance. The second statement holds for the same reason.

We are now ready for the proof of the main theorem, which we restate below for convenience.

Theorem 1 (Coverage of [Algorithm 1](#)). *Fix level $\alpha \in (0, 1)$. Let $\{(x_i, y_i)\}_{i=1}^n$ be i.i.d. samples drawn from the joint distribution $P_{X,Y}$ and $\{\tilde{x}_j\}_{j=1}^N$ be i.i.d. samples drawn from the marginal P_X . Then, under [Assumption 1](#) and as $n \rightarrow \infty$, the output of [Algorithm 1](#)—restricted to at most L leaf nodes—satisfies:*

$$\Pr \left[\mu \in \left[\hat{\mu}_T - z_{1-\alpha/2} \hat{\sigma}, \hat{\mu}_T + z_{1-\alpha/2} \hat{\sigma} \right] \right] \geq 1 - \alpha - \sqrt{\frac{2L \cdot \log(d \cdot n)}{n}} - \frac{1}{(n \cdot d)^L}.$$

Proof of Theorem 1. Applying [Theorem 8](#) by setting $\delta = \frac{1}{(n \cdot d)^{2L}}$ and applying union bound over the $(n \cdot d)^L$ possible trees in \mathcal{T}_L ([Theorem 7](#)), we get that with probability at least $1 - \frac{1}{(n \cdot d)^L}$, for any tree $T \in \mathcal{T}_L$:

$$\sigma_T \sqrt{1 - 2\sqrt{\frac{2L \cdot \log(d \cdot n)}{n}}}.$$

For the rest of the proof we condition on this event. Let $T^* \in \mathcal{T}_L$ be the selected tree from [Algorithm 1](#), in which case $\hat{\mu}_T = \hat{\mu}_{T^*}$ and $\hat{\sigma} = \hat{\sigma}_{T^*}$ (c.f. paragraph **Constructing Confidence Intervals** in [Section 4.1](#)). As $n \rightarrow \infty$, by [Theorem 8](#):

$$\begin{aligned} & \Pr \left[\mu \in \left[\hat{\mu}_T - z_{1-\alpha/2} \hat{\sigma}_{T^*}, \hat{\mu}_T + z_{1-\alpha/2} \hat{\sigma}_{T^*} \right] \right] \\ & \geq \Pr \left[\mu \in \left[\hat{\mu}_T - z_{1-\alpha/2} \sigma_{T^*} \sqrt{1 - 2\sqrt{\frac{2L \cdot \log(d \cdot n)}{n}}}, \hat{\mu}_T + z_{1-\alpha/2} \sigma_{T^*} \sqrt{1 - 2\sqrt{\frac{2L \cdot \log(d \cdot n)}{n}}} \right] \right] \\ & = 2\Phi \left(z_{1-\alpha/2} \cdot \sqrt{1 - 2\sqrt{\frac{2L \cdot \log(d \cdot n)}{n}}} \right) - 1 \end{aligned}$$

where in the first inequality we used that:

$$\begin{aligned} & \left[\hat{\mu}_T - z_{1-\alpha/2} \hat{\sigma}_{T^*}, \hat{\mu}_T + z_{1-\alpha/2} \hat{\sigma}_{T^*} \right] \\ & \supseteq \left[\hat{\mu}_T - z_{1-\alpha/2} \sigma_{T^*} \sqrt{1 - 2\sqrt{\frac{2L \cdot \log(d \cdot n)}{n}}}, \hat{\mu}_T + z_{1-\alpha/2} \sigma_{T^*} \sqrt{1 - 2\sqrt{\frac{2L \cdot \log(d \cdot n)}{n}}} \right], \end{aligned}$$

and in the second equality we used that $\hat{\mu}_{T^*}$ is distributed according to normal distribution ([Theorem 8](#)), and Φ is the CDF of $\mathcal{N}(0, 1)$. In the following claim we relate

$$\Phi \left(z_{1-\alpha/2} \cdot \sqrt{1 - 2\sqrt{\frac{2L \cdot \log(d \cdot n)}{n}}} \right)$$

with α .

Claim 6. For any constant $0 \leq C \leq 1$, $\Phi(C \cdot z_{1-\alpha/2}) \geq 1 - \frac{\alpha}{2} - \frac{1-C}{4}$

Proof. By concavity of Φ we have:

$$\begin{aligned}\Phi(C \cdot z_{1-\alpha/2}) &= \Phi(C \cdot z_{1-\alpha/2} + (1-C) \cdot 0) \\ &\geq C \cdot \Phi(z_{1-\alpha/2}) + (1-C) \cdot \Phi(0) \\ &= C \cdot \left(1 - \frac{\alpha}{2}\right) + \frac{1-C}{2} \\ &= \left(1 - \frac{\alpha}{2}\right) - \frac{(1-C)(1-\alpha)}{2} \\ &\geq \left(1 - \frac{\alpha}{2}\right) - \frac{1-C}{4},\end{aligned}$$

where in the first inequality we used that $z_{1-\alpha/2}$ is the $1 - \alpha/2$ quintile of $\mathcal{N}(0, 1)$, and in the last inequality we used that $\alpha \in [0, 1]$. \square

Thus,

$$\begin{aligned}Pr\left[\mu \in \left[\hat{\mu}_T - z_{1-\alpha/2} \hat{\sigma}_{T^*}, \hat{\mu}_T + z_{1-\alpha/2} \hat{\sigma}_{T^*}\right]\right] \\ \geq 1 - \frac{1 - \sqrt{1 - 2\sqrt{\frac{2L \cdot \log(d \cdot n)}{n}}}}{2}\end{aligned}$$

By combining these two events we have that:

$$\Pr\left[\mu \in \left[\hat{\mu}_T - z_{1-\alpha/2} \hat{\sigma}, \hat{\mu}_T + z_{1-\alpha/2} \hat{\sigma}\right]\right] \geq 1 - \alpha - \frac{1 - \sqrt{1 - 2\sqrt{\frac{2L \cdot \log(d \cdot n)}{n}}}}{2} - \frac{1}{(n \cdot d)^L}$$

The proof concludes by using inequality $1 - \sqrt{1 - x} \leq x$ for $x \in [0, 1]$. \square

D Proof of Theorem 2

In this section, we show that the residual vector formed by PART estimator for linear regression is distributed asymptotically as a normal distribution.

Theorem 2. Define $V_{\mathcal{R}} = \tilde{\Sigma}^{-1} \text{Var}[x(f(x) - y) \mid x \in \mathcal{R}] \tilde{\Sigma}^{-1}$. Under [Assumption 2](#), as $n \rightarrow \infty$,

$$\hat{R}_{\mathcal{R}} \xrightarrow{d} \mathcal{N}\left(\left(\mathbb{E}[xx^T]\right)^{-1} \mathbb{E}[x(y - f(x)) \mid x \in \mathcal{R}], \frac{V_{\mathcal{R}}}{n_{\mathcal{R}}}\right),$$

and $\hat{V}_{\mathcal{R}}$ is a consistent estimator of $V_{\mathcal{R}}$.

Proof. As $n \rightarrow \infty$ and since $p_{\mathcal{R}} > 0$, this implies that $n_{\mathcal{R}} \rightarrow \infty$. Under [Assumption 2](#) and as $n_{\mathcal{R}} \rightarrow \infty$, by the CLT:

$$\hat{R}_{\mathcal{R}} = \frac{1}{n_{\mathcal{R}}} \tilde{\Sigma}^{-1} X_{\mathcal{R}}^T (Y_{\mathcal{R}} - f(X_{\mathcal{R}})) \xrightarrow{d} \mathcal{N}\left(\mathbb{E}[\hat{R}_{\mathcal{R}}], \frac{\text{Var}[\tilde{\Sigma}^{-1} X_{\mathcal{R}}^T (Y_{\mathcal{R}} - f(X_{\mathcal{R}}))]}{n_{\mathcal{R}}}\right).$$

Computing $\mathbb{E}[\hat{R}_{\mathcal{R}}]$: Observe that:

$$\begin{aligned}\mathbb{E}[\hat{R}_{\mathcal{R}}] &= \frac{1}{n_{\mathcal{R}}} \mathbb{E} \left[\tilde{\Sigma}^{-1} X_{\mathcal{R}}^T (Y_{\mathcal{R}} - f(X_{\mathcal{R}})) \right] \\ &= (\mathbb{E}[xx^T])^{-1} \mathbb{E} \left[\frac{X_{\mathcal{R}}^T (Y_{\mathcal{R}} - f(X_{\mathcal{R}}))}{n_{\mathcal{R}}} \right] \\ &= (\mathbb{E}[xx^T])^{-1} \mathbb{E} \left[x(y - f(x)) \mid x \in \mathcal{R} \right],\end{aligned}$$

where in the second equality we used that $\tilde{\Sigma} = \mathbb{E}[xx^T]$, and in the third equality we use that $\frac{X_{\mathcal{R}}^T (Y_{\mathcal{R}} - f(X_{\mathcal{R}}))}{n_{\mathcal{R}}}$ is an unbiased estimator for $\mathbb{E} \left[x(y - f(x)) \mid x \in \mathcal{R} \right]$.

Showing Consistency for $\hat{V}_{\mathcal{R}}$: Observe that:

$$\begin{aligned}\text{Var}[\hat{R}_{\mathcal{R}}] &= \text{Var} \left[\frac{\tilde{\Sigma}^{-1} X_{\mathcal{R}}^T (Y_{\mathcal{R}} - f(X_{\mathcal{R}}))}{n_{\mathcal{R}}} \right] \\ &= \tilde{\Sigma}^{-1} \text{Var} \left[\frac{X_{\mathcal{R}}^T (Y_{\mathcal{R}} - f(X_{\mathcal{R}}))}{n_{\mathcal{R}}} \right] \tilde{\Sigma}^{-1} \\ &= \frac{1}{n_{\mathcal{R}}^2} \tilde{\Sigma}^{-1} \text{Var} \left[X_{\mathcal{R}}^T (Y_{\mathcal{R}} - f(X_{\mathcal{R}})) \right] \tilde{\Sigma}^{-1} \\ &= \frac{1}{n_{\mathcal{R}}} \tilde{\Sigma}^{-1} \text{Var} \left[x(y - f(x)) \mid x \in \mathcal{R} \right] \tilde{\Sigma}^{-1}.\end{aligned}$$

Folklore results imply that $\hat{M}_{\mathcal{R}}$ is an unbiased estimator for $\text{Var} \left[x(y - f(x)) \mid x \in \mathcal{R} \right]$, which implies that $\hat{V}_{\mathcal{R}}$ is an unbiased estimator for $\text{Var}[\hat{R}_{\mathcal{R}}]$. \square

E Proof of Theorem 4

In this section, we bound the bias and variance of estimate produced by [Algorithm 3](#) by using Taylor expansions around order statistics.

Additional Notation. We will now establish some additional notation that will be useful throughout this section. We will be interested in characterizing the gaps between the uniform order statistics. Define

$$\Delta_i = \begin{cases} X_1, & i = 0, \\ X_{i+1} - X_i, & 1 \leq i \leq n-1, \\ 1 - X_n, & i = n, \end{cases}$$

and let

$$S_0 = \Delta_0 \cdot r(X_1), \quad S_i = \Delta_i \cdot \frac{r(X_i) + r(X_{i+1})}{2} \text{ for } 1 \leq i \leq n-1, \quad S_n = \Delta_n \cdot r(X_n).$$

Further, let

$$I_0 = \int_0^{X_1} r(u)du, \quad I_i = \int_{X_i}^{X_{i+1}} r(u)du, \quad I_n = \int_{X_n}^1 r(u)du,$$

and observe that we may write $\mathbb{E}_{X \sim P_X}[r(X)] = \int_0^1 r(u)du = \sum_{i=0}^n I_i$. Thus, S_i is an approximation for the integral I_i over its corresponding interval. Our goal will be to bound the convergence rate of our approximation error across each interval. This will allow us to understand the bias and variance of our estimator. To proceed, we prove some helpful lemmas.

Lemma 7. *Let $\mathcal{L} = (X_i)_{i=1}^n$, where X_i is the i th order statistic from a standard uniform distribution. Then,*

$$\text{Var}_{\mathcal{L}} [\mathbb{E}_{\mathcal{U}} [\mu_{PAQ}|L]] = \text{Var}_{\mathcal{L}'} \left[X_1 \cdot r(X_1) + (1 - X_n) \cdot r(X_n) + \sum_{i=1}^{n-1} (X_{i+1} - X_i) \cdot \frac{r(X_i) + r(X_{i+1})}{2} \right]$$

Proof. To enforce boundary conditions, let $X_0 = -X_1$ and $X_{n+1} = 2 - X_n$. Then,

$$\begin{aligned} \text{Var}_{\mathcal{L}} [\mathbb{E}_{\mathcal{U}} [\mu_{PAQ}|L]] &= \text{Var}_{\mathcal{L}} \left[\mathbb{E}_{\mathcal{U}} \left[\frac{1}{N} \sum_{i=1}^N r(h(\tilde{X}_i)) | L \right] \right] \\ &= \text{Var}_{\mathcal{L}} \left[\mathbb{E}_{\tilde{X} \sim P_x} [r(h(\tilde{X})) | L] \right] \\ &= \text{Var}_{\mathcal{L}} \left[\mathbb{E}_{\tilde{X} \sim P_x} \left[\sum_{i=1}^n r(h(X_i)) \cdot \mathbb{1}[i = \arg \min_{j \in [n]} |\tilde{X} - X_j|] \right] \right] \\ &= \text{Var}_{\mathcal{L}} \left[\sum_{i=1}^n r(h(X_i)) \cdot \mathbb{E}_{\tilde{X} \sim P_x} \left[\mathbb{1}[i = \arg \min_{j \in [n]} |\tilde{X} - X_j|] \right] \right] \\ &= \text{Var}_{\mathcal{L}} \left[\sum_{i=1}^n r(h(X_i)) \cdot \Pr_{\tilde{X} \sim P_x} \left[i = \arg \min_{j \in [n]} |\tilde{X} - X_j| \right] \right] \\ &= \text{Var}_{\mathcal{L}} \left[\sum_{i=1}^n r(h(X_i)) \cdot \Pr_{\tilde{X} \sim P_x} \left[\frac{X_i + X_{i-1}}{2} \leq \tilde{X} \leq \frac{X_i + X_{i+1}}{2} \right] \right] \\ &= \text{Var}_{\mathcal{L}} \left[\sum_{i=1}^n r(h(X_i)) \cdot \left(\Pr_{\tilde{X} \sim P_x} \left[\tilde{X} \leq \frac{X_i + X_{i+1}}{2} \right] - \Pr_{\tilde{X} \sim P_x} \left[\tilde{X} \leq \frac{X_i + X_{i-1}}{2} \right] \right) \right] \\ &= \text{Var}_{\mathcal{L}} \left[\sum_{i=1}^n \frac{X_{i+1} - X_{i-1}}{2} \cdot r(X_i) \right] \\ &= \text{Var}_{\mathcal{L}} \left[\sum_{i=1}^n \frac{X_{i+1} - X_i + X_i - X_{i-1}}{2} \cdot r(X_i) \right] \\ &= \text{Var}_{\mathcal{L}} \left[X_1 \cdot r(X_1) + (1 - X_n) \cdot r(X_n) + \sum_{i=1}^{n-1} (X_{i+1} - X_i) \cdot \frac{r(X_i) + r(X_{i+1})}{2} \right], \end{aligned}$$

where the fourth equality follows by linearity of expectation, and the eighth equality follows since the CDF of $U[0, 1]$ is the identity function for $\tilde{X} \in [0, 1]$. \square

Lemma 8. *It holds that*

- *Interior* ($1 \leq i \leq n - 1$): $S_i - I_i = O(\Delta_i^3)$,
- *Left Boundary* ($i = 0$): $S_0 - I_0 = O(\Delta_0^2)$,
- *Right Boundary* ($i = n$): $S_n - I_n = -O(\Delta_n^2)$.

Proof. **Interior intervals.** We will perform a Taylor expansion around X_i for both S_i and I_i and show that the zeroth and first order terms cancel out. The expansions below are well defined since we assume $r \in C^2$. Specifically, observe that

$$\begin{aligned} S_i &= \Delta_i \cdot \frac{r(X_i) + r(X_{i+1})}{2} = \Delta_i \cdot \frac{r(X_i) + r(X_i) + r'(X_i)\Delta_i + O(\Delta_i^2)}{2} \\ &= r(X_i) \cdot \Delta_i + \frac{r'(X_i)}{2} \Delta_i^2 + O(\Delta_i^3), \end{aligned}$$

where we utilize the fact that $\max_{x \in [0, 1]} |r''(x)| \leq L_2$. Similarly,

$$\begin{aligned} I_i &= \int_{X_i}^{X_{i+1}} g(u) du = \int_0^{\Delta_i} g(X_i + t) dt \\ &= \int_0^{\Delta_i} g(X_i) + r'(X_i) \cdot t + O(t^2) dt \\ &= r(X_i) \cdot \Delta_i + \frac{r'(X_i)}{2} \cdot \Delta_i^2 + O(\Delta_i^3), \end{aligned}$$

again using the fact that the second derivative is bounded. Therefore,

$$S_i - I_i = O(\Delta_i^3).$$

Left Boundary. For the left boundary, we will perform a Taylor expansion around 0 and observe that zero order term cancels out. Specifically,

$$S_0 = \Delta_0 \cdot r(X_1) = \Delta_0 \cdot (r(0) + r'(\zeta_0) \cdot \Delta_0) = r(0) \cdot \Delta_0 + O(\Delta_0^2),$$

where $\max_{x \in [0, 1]} |r'(x)| \leq L_1$. Likewise,

$$I_0 = \int_0^{X_1} r(u) du = \int_0^{\Delta_0} r(t) dt = \int_0^{\Delta_0} r(0) + r'(\zeta_0) \cdot t dt = r(0) \cdot \Delta_0 + O(\Delta_0^2).$$

Taken together,

$$S_0 - I_0 = O(\Delta_0^2).$$

Right boundary. Analogous to the previous case, we will form a Taylor expansion around 1 and observe that the zero order term cancels out, additionally we utilize that the first derivative is bounded. Specifically,

$$S_n = \Delta_n \cdot r(Z_n) = \Delta_n \cdot (r(1) - O(\Delta_n)) = r(1) \cdot \Delta_n - O(\Delta_n^2),$$

Then,

$$I_n = \int_{X_n}^1 r(x)dx = \int_0^{\Delta_n} r(X_n + t)dt = \int_0^{\Delta_n} r(1) - O(t)dt = r(1) \cdot \Delta_n - O(\Delta_n^2).$$

So

$$S_n - I_n = -O(\Delta_n^2).$$

□

To bound the final bias and variance, we will need to understand the distribution of the gaps of the uniform order statistics. Their distribution is captured in the fact below.

Fact 2 (Gaps of Uniform Order Statistics). *Let $\Delta_0, \dots, \Delta_n$ be gaps in the relative order statistics a n -sample from a standard uniform distribution. Then, $(\Delta_0, \Delta_1, \dots, \Delta_n) \sim \text{Dirichlet}(1, 1, \dots, 1)$, where the marginal distribution for each $\Delta_i \sim \text{Beta}(1, n)$. It is well known that $\mathbb{E}(\Delta_i^p \Delta_j^q) = O(n^{-(p+q)})$ for $p, q \geq 1$.*

We now restate a prove the main theorem of this section.

Theorem 4 (PAQ Estimator, Degree-One Interpolation). *Under [Assumption 3](#) and $P_X = \mathcal{U}_{[0,1]}$, it holds that*

$$|\mathbb{E}[\mu_{PAQ}] - \mathbb{E}[Y]| = O\left(\frac{1}{n^2}\right) \quad \text{and} \quad \text{Var}(\mu_{NN}) = O\left(\frac{1}{N} + \frac{1}{n^4}\right).$$

Proof of Theorem 4. We will first prove the variance bound, which in implies that bound on the bias. By the law of total variance,

$$\text{Var}[\mu_{PAQ}] = \underbrace{\mathbb{E}_{\mathcal{L}}[\text{Var}_{\mathcal{U}}[\mu_{PAQ}|L]]}_{A} + \underbrace{\text{Var}_{\mathcal{L}}[\mathbb{E}_{\mathcal{U}}[\mu_{PAQ}|L]]}_{B}.$$

Term (A): For fixed \mathcal{L} , the $h(\tilde{x}_i)$ terms are i.i.d.. Consequently,

$$\begin{aligned} \mathbb{E}_{\mathcal{L}}[\text{Var}_{\mathcal{U}}[\mu_{PAQ}|L]] &= \mathbb{E}_{\mathcal{L}} \left[\text{Var}_{\mathcal{U}} \left[\frac{1}{N} \sum_{i=1}^N f(\tilde{X}_i) + r(h(\tilde{X}_i)) | L \right] \right] \\ &= \mathbb{E}_{\mathcal{L}} \left[\frac{\text{Var}_{\tilde{X}_i \sim P_X}[f(\tilde{X}_i) + r(h(\tilde{X}_i))] }{N} \right] \\ &= O\left(\frac{1}{N}\right), \end{aligned}$$

where the the last equality follows from that fact that $\text{Var}[Y]$ and $\text{Var}[f(X)]$ is bounded.

Term (B): We begin by observing that

$$\begin{aligned} \text{Var}_{\mathcal{L}}[\mathbb{E}_{\mathcal{U}}[\mu_{PAQ}|L]] &= \text{Var}_{\mathcal{L}} \left[\mathbb{E}_{\mathcal{U}} \left[\frac{1}{N} \sum_{i=1}^N f(\tilde{X}_i) + r(h(\tilde{X}_i)) | L \right] \right] \\ &= \text{Var}_{\mathcal{L}} \left[\mathbb{E}_{\mathcal{U}} \left[\frac{1}{N} \sum_{i=1}^N r(h(\tilde{X}_i)) | L \right] \right], \end{aligned}$$

since $\text{Var}_{\mathcal{L}}(f(X)) = 0$. Wlog assume that $X_1 \leq \dots \leq X_n$. Then, X_i is the i th order statistics from a standard uniform distribution. By [Lemma 7](#), it holds that

$$\text{Var}_{\mathcal{L}} [\mathbb{E}_{\mathcal{U}} [\mu_{\text{PAQ}} | L]] = \text{Var}_{\mathcal{L}} \left[X_1 \cdot r(X_1) + (1 - X_n) \cdot r(X_n) + \sum_{i=1}^{n-1} (X_{i+1} - X_i) \cdot \frac{r(X_i) + r(X_{i+1})}{2} \right].$$

Hence, we may then write this variance as

$$\text{Var}_{\mathcal{L}} [\mathbb{E}_{\mathcal{U}} [\mu_{\text{PAQ}} | L]] = \text{Var} \left[\sum_{i=0}^n S_i \right] = \text{Var} \left[\sum_{i=0}^n S_i - I_i \right],$$

since $\sum_{i=0}^n I_i$ is a constant. By [Lemma 8](#), we may perform a Taylor expansion to find that

$$\text{Var}_{\mathcal{L}'} \left[\sum_{i=1}^n S_i - I_i \right] = \text{Var}_{\mathcal{L}'} \left[O(\Delta_0^2) - O(\Delta_n^2) + \sum_{i=1}^{n-1} O(\Delta_i^3) \right].$$

We now employ [Definition 2](#) which implies that

$$\begin{aligned} \text{Var}[\Delta_0^2] &= \text{Var}[\Delta_n^2] = O\left(\frac{1}{n^4}\right), \\ \text{Var}(\Delta_i^3) &= O\left(\frac{1}{n^6}\right) \text{ for } 1 \leq i \leq n-1. \end{aligned}$$

So,

$$\text{Var} \left(\sum_{i=1}^{n-1} O(\Delta_i^3) \right) = O \left(\sum_{i,j} \text{Cov}(\Delta_i^3, \Delta_j^3) \right) = O(n^2 \text{Cov}(\Delta_i^3, \Delta_j^3)) = O\left(\frac{1}{n^4}\right),$$

since $\text{Cov}(\Delta_i^3, \Delta_j^3) = \frac{1}{n^2}$. To bound the other covariance terms, we observe that $\text{Cov}(X, Y) \leq \sqrt{\text{Var}(X) \text{Var}(Y)}$, hence the other covariance terms are also $O(n^{-4})$. Consequently,

$$\text{Var}(\mu_{\text{PAQ}}) = \text{Var}_{\mathcal{L}'} \left[\sum_{i=1}^n S_i - I_i \right] = O\left(\frac{1}{n^4}\right)$$

We may use this result to bound the bias of the PAQ estimator. Observe that

$$\begin{aligned} \mathbb{E}[\mu_{\text{PAQ}}] - \mathbb{E}[Y] &= \mathbb{E}_{\mathcal{L}} [\mathbb{E}_{\mathcal{U}} [\mu_{\text{PAQ}} | L] - \mathbb{E}[Y]] \\ &= \mathbb{E}_{\mathcal{L}} \left[\sum_{i=0}^n S_i - I_i \right] \\ &= O\left(\frac{1}{n^2}\right) \end{aligned}$$

to complete the proof. \square